

~~Forest-floor greenhouse gas fluxes in a subalpine spruce forest: Continuous multi-year measurements, drivers, and budgets~~ Forest-floor respiration, N₂O, and CH₄ fluxes in a subalpine spruce forest: Drivers and annual budgets

5 Luana Krebs¹, Susanne Burri¹, Iris Feigenwinter¹, Mana Gharun², Philip Meier¹, Nina Buchmann¹

¹Department of Environmental Systems Science, Institute of Agricultural Sciences, ETH Zurich, Switzerland

²Faculty of Geosciences, Institute of Landscape Ecology, University of Munster, Germany

Correspondence to: Luana Krebs (luana.krebs@usys.ethz.ch)

Abstract. Forest ecosystems play an important role in the global carbon (C) budget by sequestering a large fraction of anthropogenic carbon dioxide (CO₂) emissions and by acting as important methane (CH₄) sinks. The forest-floor greenhouse gas (GHG; CO₂, CH₄ and nitrous oxide N₂O) flux, i.e., from soil and understory vegetation, is one of the major components to consider when determining the C or GHG budget of forests. Although winter fluxes are essential to determine the annual C budget, only very few studies have examined long-term, year-round forest-floor GHG fluxes. Thus, we aimed to i) quantify ~~the~~ seasonal and annual variations of forest-floor GHG fluxes; ii) evaluate their drivers, including the effects of snow cover, timing, and amount of snow-melt, and iii) calculate annual budgets of forest-floor C and GHG fluxes for a subalpine spruce forest in Switzerland. We measured GHG fluxes year-round during four years with four automatic large chambers at the ICOS Class 1 Ecosystem station Davos (CH-Dav). We applied random forest models to investigate environmental drivers and to gap-fill the flux time series. The forest floor emitted 2340 g CO₂ m⁻² yr⁻¹ (average over four years). Annual and seasonal forest-floor ~~CO₂-emissions~~respiration responded most strongly to soil temperature and snow depth (-2.34 ± 0.20 kg CO₂-m⁻²-yr⁻¹). No response of forest-floor ~~CO₂-emissions~~respiration to leaf area index or photosynthetic photon flux density was observed, suggesting a strong direct control of soil environmental factors and a weak or even lacking indirect control of canopy biology. Furthermore, the forest-floor was a consistent CH₄ sink (-0.71 ~~-19.1~~ ± 1.8 g CH₄ CO₂-eq-m⁻² yr⁻¹), with annual fluxes driven mainly by snow depth. Winter CO₂ f~~Fluxes during winter~~ were less important for the CO₂ budget (6.0–7.3 %), while ~~they~~ winter CH₄ fluxes contributed substantially to the annual CH₄ budget (14.4–18.4 %). N₂O fluxes were very low (0.007 g N₂O ~~m⁻² yr⁻¹~~), negligible for the forest-floor GHG budget at our site. In 2022, the warmest year on record with ~~also~~ below-average precipitation at the Davos site, we observed a substantial increase in forest-floor ~~CO₂-emissions~~respiration compared to other years. The mean forest-floor GHG-C budget indicated emissions of 2317 ± 200 g CO₂-eq m⁻² yr⁻¹ (mean \pm standard deviation over four years), with ~~CO₂-respiration~~ fluxes dominating and CH₄ offsetting a small proportion (0.8 %) of the GHG-C budget. Due to the relevance of snow cover, we recommend year-round measurements of GHG fluxes with high temporal resolution.

30 In a future with increasing temperatures and less snow cover due to climate change, we expect increased forest-floor ~~CO₂-emissions~~respiration ~~even~~ at this subalpine site, with negative effects on its carbon sink ~~behaviour~~capacity.

1 Introduction

35 Carbon dioxide (CO₂), methane (CH₄), and nitrous oxide (N₂O) are the three main greenhouse gases (GHGs) driving global warming. Forest ecosystems play an important role in the global carbon (C) cycle by sequestering a large fraction of anthropogenic CO₂ emissions and by acting as an important CH₄ sink (Borken et al., 2006; Ni and Groffman, 2018; Friedlingstein et al., 2023). The GHG flux of the forest-floor, i.e., soil and understory vegetation, is one of the major components to consider when determining the C budget of forests, since soil respiration is the second largest terrestrial C flux and accounts for approximately 70 % of CO₂ losses in temperate forests (IPCC, 2021; Yuste et al., 2005). However, how forest-floor GHG fluxes will respond to climate change is still largely unknown.

40 Global warming particularly affects high latitude and high altitude forests (IPCC, 2021), altering snowfall, length and timing of snow cover as well as melting and soil freeze-thaw cycles (CH2018, 2018; Klein et al., 2016). Nevertheless, there have been very few studies that examined continuous, year-round and long-term forest-floor GHG fluxes in high latitude or high altitude forests (Barba et al., 2019; Luo et al., 2011). Unfortunately, measurements during periods with snow cover are challenging and thus often lacking due to logistical reasons, leading to winter fluxes missing even from multi-year studies (e.g., Richardson et al., 2019).

~~The forest-floor's CO₂ fluxes include involve the processes of~~ photosynthetic CO₂ uptake by plants as well as autotrophic and heterotrophic respiratory losses from plants and soils, respectively (Hanson et al., 2000). All three processes and their contributions to the total soil CO₂ fluxes depend on biotic and abiotic factors as well as their interactions. For example, ~~autotrophic soil~~ respiration is ~~mainly driven by plant activity and hence linked to~~ coupled to canopy photosynthesis and ~~thus to incoming radiation solar energy (Högberg et al., 2001; Janssens et al., 2001), whereas, heterotrophic respiration is but also~~ strongly controlled by soil conditions (i.e., soil temperature and moisture), substrate availability, and the microbial community (e.g., Janssens et al., 2001; Scott-Denton et al., 2006; Högberg et al., 2001). Furthermore, winter dynamics can impact soil respiration rates through changes in snow cover, soil freezing and thawing cycles (Reinmann and Templer, 2018; Schindlbacher et al., 2007). Especially, freeze-thaw events have recently been the focus of research because they cause abrupt changes in biophysical soil conditions which can alter autotrophic and heterotrophic soil respiration rates (Song et al., 2017).

55 How soil respiration responds to climate change is, however, not fully clear. With increasing soil temperatures as a consequence of increasing air temperatures (Lembrechts et al., 2022), global observations and models show a globally rising trend of soil respiration over recent decades and a continuation of the increase with progressing climate change (Bond-Lamberty et al., 2018; Nissan et al., 2023). At the same time, there is evidence for a thermal optimum of ecosystem respiration over a range of different biomes, indicating a non-monotonic relationship between soil temperature and respiration (Chen et al., 2023). ~~How the two components of soil respiration respond to climate change is however subject to major uncertainties with many studies showing contradictory results. Some studies demonstrated no significant increase of soil respiration to experimental warming in forest soils (Bradford et al., 2008; Carey et al., 2016), while others observed higher soil respiration rates (Bond-Lamberty et al., 2018; Crowther et al., 2016; Karhu et al., 2014). Among those reporting higher rates, there is~~

65 ~~disagreement on whether long-term adaptation can occur. In some studies, the higher respiration rates were sustained over several years (Melillo et al., 2017), while in others they declined again to previous levels (Eliasson et al., 2005; Hartley et al., 2007).~~

Forest soils have been shown to act as an atmospheric CH₄ sink (Dutaur and Verchot, 2007). The uptake of CH₄ in ~~oxic well-aerated~~ soils ~~occurs due~~ is related to the presence of methan-~~oxidizing~~ otrophic bacteria (Saunois et al., 2020). ~~This process~~ is highly dependent on environmental factors, including soil temperature (T_{soil}), soil texture (transport of CH₄ into the soil), soil moisture (transport of CH₄ into the soil and limitation of bacterial activity), and soil nitrogen (N) content (Borken et al., 2006; Luo et al., 2013; Ni and Groffman, 2018). Furthermore, biotic factors such as plant cover can affect CH₄ ~~consumption~~ uptake of the forest floor through the presence of *Sphagnum* moss species which are inhabited by methane-oxidizing bacteria (Basiliko et al., 2004). Generally, in temperate forests, CH₄ uptake increases in warmer and drier soils (Borken et al., 2006; Ni and Groffman, 2018). Winter dynamics further impact CH₄ fluxes, with frozen soil and snow cover affecting microbial activity and gas transport (Blankinship et al., 2018; Borken et al., 2006). Understanding the drivers of forest-floor CH₄ fluxes, including the complex interplay between biotic and abiotic factors, is vital for accurately modeling and predicting the role of forest ecosystems in the global CH₄ cycle.

Moreover, the forest-floor can act as a source or sink of N₂O (Chapuis-Lardy et al., 2007; Goldberg et al., 2010). Soil temperature, soil moisture, and N availability significantly influence N₂O fluxes through regulating ~~the~~ microbial processes which are mainly responsible for N₂O production in soils, i.e., nitrification and denitrification (Schaufler et al., 2010). High N₂O emission rates in temperate forests have been found under warm and moist conditions (Luo et al., 2013). Furthermore, ~~studies have revealed that~~ high N₂O emissions occur during freezing-thawing cycles and rewetting events, when abrupt changes in temperature and moisture conditions promote microbial activity and thus the release of N₂O (Goldberg et al., 2010; Papein and Butterbach-Bahl, 1999; Liu et al., 2018; Butterbach-Bahl et al., 2013). Understanding the dynamics of these processes and drivers, particularly during freezing-thawing cycles, is crucial for estimating N₂O emissions from forests.

In this study, we investigated combined measurements of forest-floor CO₂ respiration, CH₄ and N₂O ~~forest floor~~ fluxes in a subalpine Norway spruce forest (Davos, CH-Dav, ICOS Class 1 Ecosystem station), in response to biotic and environmental drivers, based on four years of continuous-year-round measurements (2017, 2020-2022). Our objectives were to i) quantify seasonal and annual variations in climate variables and forest-floor respiration CO₂, CH₄ and N₂O fluxes; ii) evaluate the drivers of forest-floor GHG fluxes, including effects of snow cover, timing and amount of snow-melt; and iii) calculate the annual budgets of forest floor GHG fluxes. We hypothesized that the forest floor is a source of CO₂ throughout the years, with large seasonal variability due to the temperature sensitivity of respiratory processes, but very low N₂O emissions due to the overall low N supply at the site. In contrast, we expected that the forest floor is a net sink of CH₄, with soil temperature and snow dynamics being important drivers due to their impact on microbial activity and diffusion rates between soil and atmosphere. Thus, we expected the highest respiratory fluxes and CH₄ uptake in 2022, an exceptionally warm year at our site. Overall, we anticipated the forest-floor GHG budget being mainly determined by respiration fluxes, with CH₄ uptake only slightly offsetting the respiratory CO₂ losses and N₂O emissions being negligible.

2 Methods

100 2.1 Study site

The study site is a subalpine evergreen coniferous forest, located in the eastern Swiss Alps at ~~a mean~~ altitude of 1640 m a.s.l. (Davos Seehornwald; CH-Dav; 46°48'55.2" N, 9°51'21.3" E). The total annual precipitation is 876 mm, and the mean annual temperature is 4.3 °C (1997–2022). The site is certified as ICOS (Integrated Carbon Observation System) Class 1 Ecosystem station for eddy-covariance flux measurements since 2019. The dominant species is Norway spruce (*Picea abies* (L.) Karst), with an average tree height of 18 m (max. 35 m), and a mean tree age of approx. 100 years (with some ~~specimens~~ ~~trees~~ reaching over 300 years). Understory vegetation covers about 30 % of the surface and is mainly composed of blueberry (*Vaccinium myrtillus* and *Vaccinium gaulterioides*) and mosses (*Sphagnum* sp. Ehrh. ~~and~~ *Hylocomium splendens*). CH-Dav is a sustainably managed forest according to the Swiss National Forest Protection Law (1876; Tschopp, 2012). The soil types are chromic cambisols (L, F, H layers with 1 cm, 2 cm, and 1.5 cm thickness, respectively; A, B(h), B(fe), B, and (B)Cv horizons with 0–4 cm, 4–12 cm, 12–45 cm, 45–70 cm, and > 70 cm depth, respectively) and rustic podzols (L, F, H layers with 1 cm, 3 cm, and 7 cm thickness, respectively; Ah, (A)E, Bfe, BCv, and (B)Cv horizons with 0–3 cm, 3–10 cm, 10–40 cm, 40–80 cm, and > 80 cm soil depth, respectively; ~~-(FAO classification; Jörg, 2008; Tab. 4).~~ Soil texture ranges from sand to sandy loam (Jörg, 2008). Soil bulk density at 5 cm depth of mineral soil is between 0.27–0.35 g cm⁻³ (Saby et al., 2023). Soil C and N stocks (0 to 60 cm depth) are on average 142.3 and 5.1 t ha⁻¹, respectively (Jörg, 2008).

115 2.2 Chamber flux measurements

2.2.1 Chamber set-up ~~and tests~~

Forest-floor ~~CO₂ respiration~~, CH₄ and N₂O fluxes were measured during the years 2017 and 2020–2022 using a fully automated system with four chambers (FF1 to FF4), distributed within an area of 3600 m² in the forest ~~to~~, representative for the eddy-covariance footprint. Concentrations of CO₂, CH₄ and N₂O were measured with a Dual Laser Trace Gas Analyzer (TILDAS, Aerodyne Research, Billerica, USA) since 2017. ~~To ensure high measurement quality, laser temperatures and tuning rates were adjusted on a regular basis. After the measurement campaign in 2017, the TILDAS was sent to Aerodyne for maintenance and repair (new N₂O laser source); measurements of all three GHG were resumed in fall 2019. Since In January 2021, the N₂O laser broke, thus N₂O these measurements were reduced to measure CH₄ only, due to failure of one of the lasers stopped. In addition, s~~Since November 2019, CO₂ concentrations in the chambers were ~~also~~ measured with an infrared gas analyzer (LI-840, LI-COR Biosciences, Lincoln NE, USA). For the year 2020, CO₂ chamber measurements from both ~~QCL-TILDAS~~ and ~~LI-840~~ were available and used for further analyses (see below). ~~For 2021 and 2022, only the IRGA CO₂ measurements were used.~~

Chambers were designed according to Brümmer et al. (2017), following the ICOS RI protocol for chamber measurements (Pavelka et al., 2018). The ~~large~~ opaque PVC chambers (~~white surfaces to increase albedo~~) rested on aluminum frames, ~~and~~ ~~were~~ inserted 10 cm ~~into~~ the soil, sealed with EPDM (ethylene propylene diene monomer) gaskets. ~~Their large size, and had~~

~~the dimension of~~ (75 cm x 75 cm x 50 cm height, ~~(thus approx. 281 dm³)~~ allowed to reduce edge effects as much as possible. ~~They~~ Chambers were equipped with a pressure vent, as well as air temperature and pressure sensors (BME280, Bosch Sensortec GmbH, Reutlingen, Germany). During the winter periods with snowfall, extension frames (2 x 50 cm height) allowed to increase their chamber height. A 17 Watt geared electric motor (80807021, Crouzet, Valence, France) was used to move the entire PVC chamber vertically and horizontally by about 190 cm and 70 cm, respectively (Fig. A.1). One webcam per chamber allowed remote observation of the operation and estimates of snow cover and depth (see below). Since the vegetation inside the chamber frames was not cut, the chamber set-up measured forest-floor GHG fluxes (and not only soil fluxes). Due to their opaque material, no understory photosynthesis was measured with the chambers. Soil and vegetation cover inside the chambers (differentiated into three plant functional types: moss, grass, blueberry) were assessed visually in June 2022, when also ~~the~~ leaf area index (LAI) of the spruce forest was measured using digital photography above the chamber locations (Fuentes et al., 2008). One chamber cycle lasted 10 minutes~~cycle fit within 10 minutes, with 3 minutes for the actual measurement period (when chamber resided on the frame, i.e. was fully closed), 3.5 minutes for closing, and 3.5 minutes for opening including closing and opening operations~~ the chambers (slow upward and sideward movement was controlled by an Arduino Ethernet), with an actual measurement period of 180 s when the chamber resided on the frame. Thus, chambers were fully closed for 48 minutes per day (i.e., 3.3 % of the day), during which rainfall was fully excluded. If we added the time when the chambers were hovering directly over the frame (about 4 minutes per cycle), the chambers would be closed for a maximum of 7 minutes per chamber cycle (i.e., 7.8 % of the day). But this is a rather conservative estimate of rainfall exclusion, since rain not always falls vertically, and throughfall is typically much less than bulk precipitation due to canopy interception. Together with further tests on potential chamber effects, i.e., SWC inside vs. outside for two chambers and four years; T_{soil} inside vs. outside for four chambers and three years (see Appendix, Figs. A.2-4), we concluded that our chamber design and closure duration avoided potential effects on environmental conditions as much as possible.

During the 10 min cycles, concentrations were measured continuously once per second. The air from the chamber was fed to the gas analyzers in 6 mm OD tubing (Synflex 1300, Eaton, Dublin, Ireland) and pumped back to the chamber, forming a closed system. Tube lengths between chamber and instrument ranged between 49–85 m, and the flow rate ranged between 0.9–1.0 slpm. We determined the time lags for the arrival of gas in the instrument based on the change in chamber status (fully open, fully closed) and max. CO₂ concentrations measured. Switching of the air stream between ~~the~~ different chambers and ~~the~~ gas analyzers was accomplished using rotary selector valves (Valco Selectors, VICI AG International, Schenkon, Switzerland). Chamber cycles (lasting app. 1 h for four chambers) were repeated every ~~three~~ 3 hours for each gas analyzer individually, leading to ~~total~~ a total of 16 cycles per chamber and day (eight per gas analyzer). Chambers H leakage tests of all four chambers were performed in 2019. Variations caused by possible leakage were below 3% of the measured flux, as required by the ICOS RI protocol (Pavelka et al., 2018).

Tab. 1: Site characteristics of the four chambers (FF1 to FF4). Annual means and standard deviations are shown for soil temperature (T_{soil}) and water filled pore space (WFPS) at 5 cm, soil depth, and days with snow cover. LAI, soil, and vegetation cover inside each

chamber were determined in June 2022. Soil data (bulk density, pH, C and N stocks in the topsoil, i.e., litter, organic material layers, and 0–20 cm depth of mineral soil) were taken from Jörg (2008).

Site characteristics	FF1	FF2	FF3	FF4	Mean
T_{soil} at 5cm (°C)					
2017	4.44 ± 4.67	4.16 ± 4.84	4.29 ± 4.86	4.56 ± 4.52	4.36 ± 0.17
2020	4.66 ± 4.32	4.40 ± 4.46	4.46 ± 4.34	4.87 ± 4.15	4.60 ± 0.22
2021	4.18 ± 4.25	3.80 ± 4.48	3.74 ± 4.84	4.26 ± 4.20	3.99 ± 0.26
2022	5.15 ± 4.70	4.83 ± 4.96	4.70 ± 5.38	5.18 ± 4.61	4.97 ± 0.24
WFPS at 5 cm (%)					
2017	20.1 ± 5.09	17.2 ± 4.30	21.3 ± 6.82	22.5 ± 7.42	20.3 ± 2.27
2020	15.9 ± 2.88	15.5 ± 3.85	9.8 ± 0.69	23.9 ± 9.55	16.3 ± 5.79
2021	16.8 ± 3.88	14.5 ± 3.88	11.8 ± 4.45	25.0 ± 10.5	17.0 ± 5.70
2022	15.1 ± 4.19	12.7 ± 3.27	10.4 ± 3.56	21.3 ± 7.16	14.9 ± 4.70
Snow depth (cm)					
2017	5.8 ± 8.4	6.4 ± 9.8	4.5 ± 6.4	3.9 ± 6.2	5.1 ± 1.2
2020	4.3 ± 7.0	8.6 ± 12.1	4.2 ± 7.0	3.5 ± 6.0	5.2 ± 2.3
2021	17.6 ± 25.0	22.2 ± 29.5	14.6 ± 22.7	14.8 ± 21.0	17.3 ± 3.6
2022	5.1 ± 9.3	8.3 ± 14.1	6.1 ± 11.7	4.9 ± 9.5	6.1 ± 1.6
Days with snow cover					
2017	152	159	152	148	153 ± 5
2020	126	142	123	117	127 ± 11
2021	172	189	161	169	173 ± 12
2022	138	145	134	132	137 ± 6
Leaf area index (LAI)					
	2.9	4.2	3.1	2.9	3.3 ± 0.6
Soil cover inside chamber (%)					
bare soil	0	50	70	0	30 ± 36
moss	90	50	20	90	63 ± 34
grass	5	1	0	0	2 ± 2
<i>Vaccinium</i>	60	0	10	30	25 ± 26
Bulk density at 5 cm (g cm⁻³)					
	0.27	0.35	0.32	0.35	0.32 ± 0.04
pH					
	2.8–3.1	3.0–3.4	2.8–3.1	3.0–3.4	
C stock (t/ha)					
	93.5	147.7	135.4	105.8	120.6 ± 25.2
N stock (t/ha)					
	3.54	5.74	4.47	3.52	4.32 ± 1.05

2.2.2 Data processing and quality assessment

The concentration increase in the chamber headspace over time was used to determine the respective flux F using Eq. (1):

$$F = \frac{\frac{\partial C}{\partial t} V \frac{m}{A} \frac{p}{V_m} \frac{T_0}{p_0} \frac{T}{T_0}}{m} \quad (1)$$

where $\frac{\partial C}{\partial t}$ is the concentration change over time (mol mol⁻¹ s⁻¹), V the actual chamber volume (m³), A the forest-floor area within the chamber frame (m²), m the molecular mass (dimensionless), V_m the molar volume (m³ mol⁻¹) of the respective gas,

p the mean chamber pressure (Pa), p_0 the standard pressure (1013.25 Pa), T_0 the standard temperature (273.15 K), and T the mean chamber temperature (K). We accounted for the varying chamber volume due to snow depth and additional extension frames installed during winter. Thus, the actual chamber volume was calculated using Eq. (2):

$$V = A \times (h_{\text{chamber}} + h_{\text{frame}} - h_{\text{snow}}) \quad (2)$$

where h_{chamber} is the height of the chamber, h_{frame} the height of the extension frame(s), and h_{snow} the snow depth. We fitted a linear regression to the change in concentration of the respective gas over time ($\frac{\partial C}{\partial t}$) during the closed period of the chamber (180 s), excluding the first 20 s after closing. The R^2 of the fit was later used for the quality assessment and filtering of the calculated fluxes (see below). A positive flux means release from the forest floor to the atmosphere, and a negative flux indicates uptake by the forest floor.

The quality of the calculated fluxes was ensured by removing negative CO_2 fluxes (Step 1), removing outliers (Step 2, despiking), and applying a filter based on R^2 for CO_2 and CH_4 and based on root mean square error (RMSE) for N_2O . (Step 3).

These three steps were applied to each chamber and GHG separately. In more detail: (1) We excluded ~~any~~ negative CO_2 fluxes (about 2 % of all fluxes). (2) We then despiked (i.e., removed outliers) the flux data set with a running mean algorithm using a width of 30 days. Step 2 removed 0.2 %, 0.7 % and 1.2 % of CO_2 , CH_4 and N_2O fluxes, respectively. (3) For CO_2 and CH_4 fluxes, we analyzed data separately for each gas, each chamber, as well as ~~For the~~ growing period (May to November) ~~and the~~ vs. dormant period (December to April), and based the quality assessment on R^2 values. ~~separately, w~~We removed fluxes with a R^2 value below the 10th percentile of all R^2 values in the respective period (except if $R^2 > 0.9$), to avoid setting a fixed

threshold for an acceptable R^2 . ~~These three steps were applied to each chamber and GHG separately.~~ The 10th percentile of R^2 values ranged from 0.0021 to 0.99, being lower during the dormant compared to the growing period (Tab. A.1). Step 3 excluded 6 % and 9 % of CO_2 and CH_4 fluxes, respectively. and particularly for ~~For~~ N_2O fluxes, we separated data of the two years available (2017, 2020) to account for the replacement of the N_2O laser source in 2019 and based the quality assessment on the RMSE (due to the low magnitude of the N_2O fluxes). N_2O fluxes with an RMSE below the 10th percentile of all RMSE, which were 0.13 and 0.03 for 2017 and 2020, respectively, were removed (Tab. 2). Step 3 excluded 25 % of all N_2O fluxes. Furthermore, for N_2O , we estimated a minimum reliable flux with the specifications of the TILDAS instrument (precision of 0.03 ppb) and the closure time, i.e., any change of N_2O concentrations in the chamber headspace during the measurement period had to be > 0.06 ppb (McManus et al., 2006) or > 29.1 nmol N_2O m^{-2} h^{-1} .

Tab. 2: 10th percentiles of R^2 values from linear regressions used for flux calculations per gas, given separately for each chamber (FF1 to FF4) and growing and dormant periods. Percentiles were applied as quality thresholds.

Gas	Period	FF1	FF2	FF3	FF4
CO ₂	growing period	0.97	0.98	0.98	0.99
	dormant period	0.35	0.48	0.47	0.68
CH ₄	growing period	0.92	0.96	0.92	0.93
	dormant period	0.41	0.26	0.21	0.61
N ₂ O	growing period	0.022	0.001	0.001	0.003
	dormant period	0.042	0.002	0.003	0.002

Initially Overall, the initial time series consisted of 40'426-38'103 CO₂ (in 2020 from ~~both two~~ gas analyzers), 2734'998503 CH₄ and 13'29144'309 N₂O flux measurements over the four years. After the quality checks described above, 37'596-34'938 CO₂ (92.3 %), and 26'565-25'083 CH₄ (91.83 %), and 9'823 N₂O (74 %) flux measurements remained, which resulted in 4446, and 3972, and 1755 daily means, respectively. ~~Due to Step 3, we excluded the forest floor N₂O fluxes from further driver and budget analyses.~~

2.2.3 Static chamber measurements

In order to check for the validity of our N₂O flux measurements using the automatic chambers, we performed N₂O measurements using static chambers (dimensions of d = 30 cm and h = 30 cm; ~~(Hutchinson and Mosier, 1981)~~). We used eight static chambers, i.e., four chambers next to the automatic chambers, and four chambers placed randomly within the research area. Soil collars were installed two weeks prior to the first measurement campaign. Four rounds of measurements were done on two days in October 2023 (n=32), when soil temperature was between 5.5-12 °C, well above the long-term mean, and when WFPS at 5 cm depth were on average 13.1 %, favoring microbial activities. Three collars were irrigated between the first and second measurement round on the two days to simulate a heavy rainfall event, favoring denitrification. We left the chambers closed for 1 h and sampled air in the headspace every 20 min. Sampling and flux calculations were done as described in ~~(Barthel et al., (2022))~~. All gas samples were analyzed at ETH Zurich for N₂O mole fraction using gas chromatography (456-GC, Scion Instruments, UK).

2.3 Environmental data

Each of the chambers had measurements of soil water content (SWC; EC-5, Decagon Devices Inc.) and T_{soil} (107, Campbell Scientific Ltd.) at 5 cm soil depth in close vicinity (< 2 m away from the chamber). To account for potential drivers of canopy photosynthesis modulating forest-floor fluxes, photosynthetic photon flux density (PPFD; PAR LITE, Kipp & Zonen), air temperature (TA; HygroClip HC2-S3, Rotronic AG), and precipitation (PREC; 1518H3, Lambrecht Meteo GmbH) data were used as well, measured at the tower above the tree canopy at 35 m height (precipitation measured at 25 m height).

We calculated water-filled pore space (WFPS) from the ~~soil water content (SWC)~~ measurements using Eq. (2):

$$WFPS = \frac{SWC}{1 - \frac{BD}{PD}} \times 100 \quad (2)$$

Bulk density (BD) was calculated using the data from a soil sampling campaign done in July 2018 according to ICOS RI standards (Arrouays et al., 2018; Saby et al., 2023). Soil data were used from soil profiles closest to the respective chambers (in total, data from six profiles were used). Particle density (PD) was assumed to be constant at 2.65 g cm^{-3} (Danielson and Sutherland, 2018). ~~M~~The mean daily snow cover and snow depth per chamber ~~was-were~~ derived from webcam images using a custom-made python image analysis tool, deriving snow depth from a scale installed in vicinity to each chamber within the image section.

2.4 Statistical analyses

2.4.1 Driver analysis

235 We used conditional random forests (RF) to model daily forest-floor ~~respiration~~ CO_2 and CH_4 fluxes (based on all years and chambers) and investigated their environmental drivers. Due to the low N_2O fluxes, we excluded them from the RF analyses. We selected predictors which were known from the literature, i.e., daily averages of T_{air} , T_{soil} at 5 cm depth, WFPS at 5 cm depth, and PPFD as well as their one- and four-day leads (meaning that we shifted the variables forward in time by one and four days). Furthermore, we added snow depth and changes in snow depth from one day to another (Δ snow depth) to the predictor set. To account for factors which could explain differences in ~~the~~-GHG fluxes among ~~the~~-chambers, we included several chamber-specific characteristics (Tab. A.12), i.e., ~~the~~-LAI, ~~the~~-bare soil fraction in the chambers, and ~~the~~-total C and N stocks in the topsoil (litter, organic ~~material~~-layers, ~~and~~ 0–20 cm depth of mineral soil). We applied the function *cforest* from the R-package “party” which can deal with highly correlated predictor variables (v1.3.10; Strobl et al., 2008, 2007). Prior to model development, predictors and target variables were centered and scaled using the “caret” *preProcess* function, which
245 brings all variables and measurements from different sensors and locations into the same range, improving performance of the RF models (v6.0.93; Kuhn, 2008). The hyperparameter fitting was done using the train function from the R-package “caret” (see Appendix for final model set-up) using 10-fold cross-validation. The assessment of driver importance in the RF model was done using the R package “permimp” which accounts for correlated variables within the predictor set (v.1.0.2; Strobl et al., 2007; Debeer and Strobl, 2020; Debeer et al., 2021). The calculated values for driver importance were rescaled to values
250 between 0 and 1 using a min-max normalization.

We developed RF models separately for daily CO_2 and CH_4 fluxes ($N = 4446$ and 3972 , respectively). The training of the RF was done using only a fraction of the data set (70 %). The remaining 30 % of the data set was used as test dataset to evaluate model performance. Centering and scaling were done separately for training and test datasets to avoid data leakage. The performance of ~~the~~-RF models was assessed using R^2 and ~~random-mean-square-errors~~-(RMSE). During model development,
255 we tested several different predictor sets. Furthermore, to optimize the models and to evaluate the robustness of model results, we evaluated the RF models trained on data sets separated by year of measurement or by chamber, and compared their accuracy to the model that was built using data from all years and all chambers. In total, 17 predictor variables entered the models (including the leads). RF models were also trained on seasonal data (i.e., spring, summer, autumn, winter; defined according

to the meteorological definition) to investigate differences in drivers among ~~the~~ seasons. For ~~the~~ seasonal RFs, we used the same predictor sets as for the RFs developed on the ~~entire multi-year~~ data set. We calculated partial dependence (PD) plots of ~~the~~ conditional RFs using the “moreparty” package (v0.3.1; Robette, 2023) which is based on the “pdp” package (v0.8.1; Goldstein et al., 2015; Greenwell, 2017) to assess ~~the~~ relationships between the four most important predictors and the predictions. The PD ~~was~~ calculated as the change in the average predicted value, while the predictor ~~at of~~ interest ~~is~~ was varied over its marginal distribution.

2.4.2 Flux gap-filling and budget calculations

The gap-filling of CO₂ and CH₄ fluxes was done using the RF models ~~developed described~~ above. Missing values in the predictor variables (gap length < 3 days) were linearly interpolated using the R package “chillR” (v0.72.8, Luedeling and Fernandez, 2022). The gap-filled flux data were then used to calculate ~~the annual budgets of forest-floor GHG-C fluxes budgets~~ per chamber. Since we estimated the annual forest-floor ~~GHG-C~~ budget for the study area, we reported the mean over the four chambers. To be able to compare CO₂ and CH₄ budgets, we converted the CH₄ budgets into CO₂-equivalents (CO₂-eq) using the 100-year global warming potential of methane of 27 (IPCC, 2021).

In addition, we modeled the daily ~~CO₂ forest-floor respiration~~ fluxes using a Q₁₀ model according to Eq. (3):

$$R_S = R_{ref} \times Q_{10}^{\frac{T_{soil} - 10}{10}} \quad (3)$$

where R_{ref} is the modeled R_S at ~~a~~ T_{soil} of 10°C, and Q₁₀ is the temperature sensitivity. We developed one model for the full dataset (all years and all four chambers together). The annual budgets calculated with the Q₁₀ modeled fluxes were then compared to the annual budgets from the RF gap-filling. All statistical analyses were performed using R Statistical Software (v4.2.0, R Core Team, 2022).

3 Results

3.1 Seasonal and interannual variability of environmental conditions and GHG fluxes

The seasonal courses of T_{air} and T_{soil} were very pronounced during the four years of the study, with highest temperatures in July and August, and lowest temperatures in January (Fig. 1a). All years showed highly variable WFPS with large differences among chambers (i.e., up to 35 % difference; Fig. 1b), ~~with and~~ highest ~~WFPS~~ values during the snowmelt period, i.e., March to May. While the snow-covered periods usually started in November and lasted until April or May (Fig. 1c), the snow depths were much higher during winter 2020/2021 (reaching snow depths of over 1 m) compared to the other winters. Overall, the year 2022 was ~~by far~~ the warmest year ever recorded at the Davos research site ~~so far~~, with an annual mean T_{air} of 5.6 °C (vs. the long-term mean of 4.3 °C; station data 1997–2022). Accordingly, annual mean T_{soil} at 5 cm was highest in 2022 for all chambers (annual mean T_{soil} over all chambers was 5.0 °C; Tab. ~~A.12~~). At the same time, precipitation in 2022 was low (773

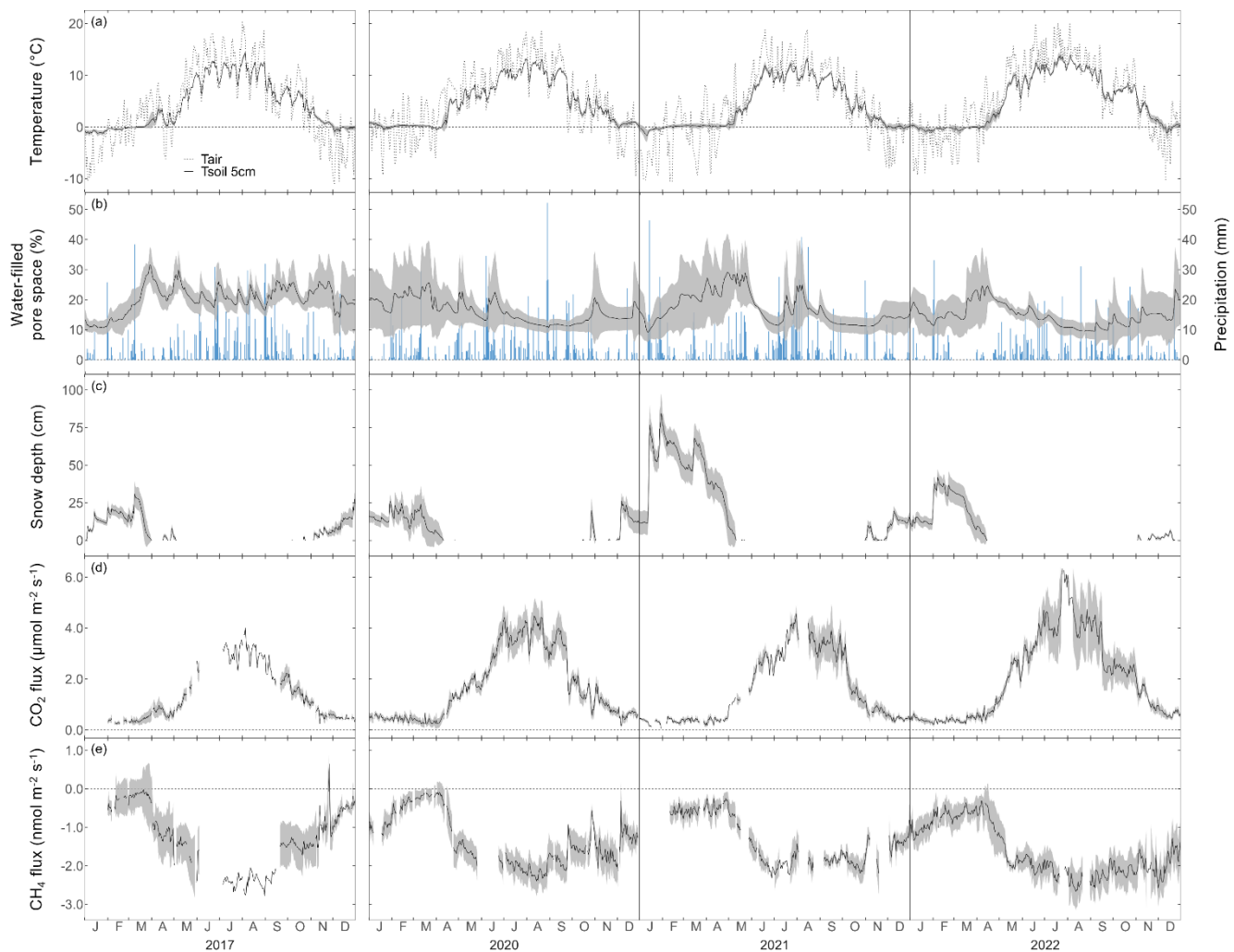
mm vs. long-term mean of 876 mm; station data 1997–2022), which led to comparably dry soil conditions (annual mean WFPS over all chambers was lowest in 2022 ~~(with 14.9 %) compared to that of the other years~~).

290 ~~On the one hand,~~ The forest floor at the Davos Seehornwald site was a source of CO₂ during all four years, independent of the season (Fig. 1d). Typically, forest-floor ~~CO₂ respiration~~ fluxes were very low in winter (mean CO₂ flux ± standard deviation (SD): 0.46±0.14 μmol m⁻² s⁻¹), increased in spring after the snow-melt, and reached their maximum values in June to September (mean CO₂ flux over all years ~~of~~: 3.50±0.84 μmol m⁻² s⁻¹). Lowest forest-floor ~~CO₂ emissions~~ ~~respiration~~ ~~were~~ ~~was~~ measured in January 2021 (min. CO₂ flux ~~of~~: 0.06 μmol m⁻² s⁻¹), highest ~~CO₂ respiratory~~ fluxes were observed in July 2022 (max. CO₂ flux ~~of~~: 6.54 μmol m⁻² s⁻¹).

295 ~~On the other hand~~ ~~Moreover~~, the forest floor was a consistent sink for CH₄, despite large short-term variations (days to weeks; Fig. 1e) and a few short peaks of CH₄ emissions in winter and spring. Seasonality of forest-floor CH₄ fluxes was very pronounced, with highest uptake in summer (mean CH₄ flux ~~of~~: -2.11±0.28 nmol m⁻² s⁻¹), and still high CH₄ uptake rates during autumn and early winter (October to December; most clearly seen in 2022). ~~With increasing duration of winter (March~~ ~~January~~ ~~to March~~; Fig. 1e), the CH₄ sink strength ~~further~~ ~~decreased~~, ~~with~~ ~~the~~ lowest CH₄ uptake ~~was~~ measured in ~~the~~ ~~months~~ ~~of~~ ~~February~~ ~~to~~ ~~March~~ (mean CH₄ flux ~~of~~: -0.4417±0.2207 nmol m⁻² s⁻¹). ~~With increasing duration of winter (March to May; Fig. 1e), the~~ ~~CH₄ sink strength further~~ ~~decreased~~. However, ~~at the end of winter~~ ~~after~~ ~~snowmelt~~, between April and end of May (depending on the year), CH₄ uptake rates increased sharply.

300 ~~Based on quality check 3, we did not consider the N₂O fluxes any further. The decision was driven by the observed low 10th percentiles of the R² values (Tab. 2), which indicated that the flux calculations frequently failed to yield satisfactory fits due to very low forest floor N₂O fluxes (Appendix Fig. A.1), often below the minimum detectable flux of N₂O. This minimum reliable flux was estimated with the specifications of the TILDAS instrument (precision of 0.03 ppb), i.e., any change of N₂O concentrations in the chamber headspace during the measurement period had to be > 0.06 ppb (McManus et al., 2006) or > 29.1 nmol N₂O m⁻² h⁻¹.~~

310



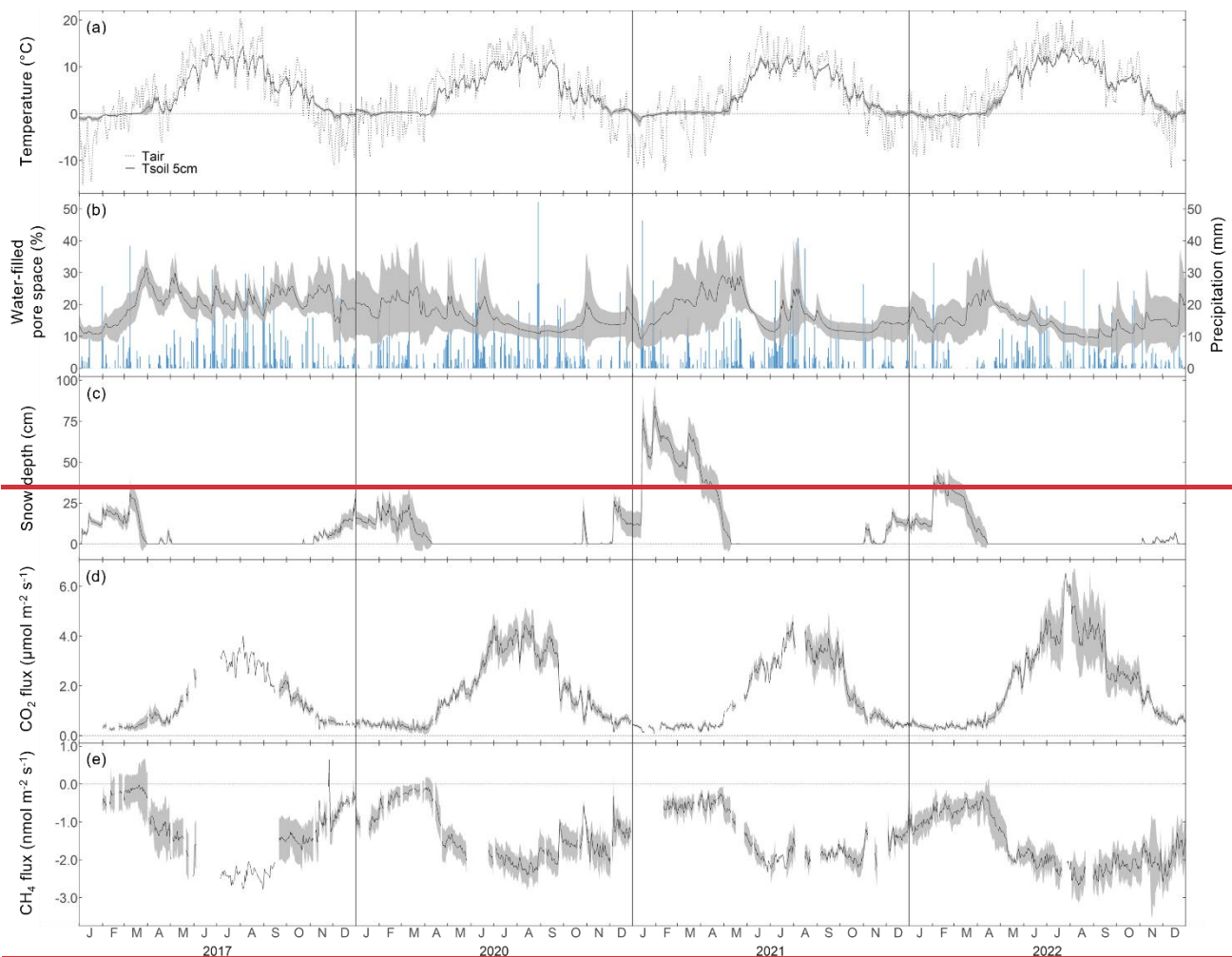
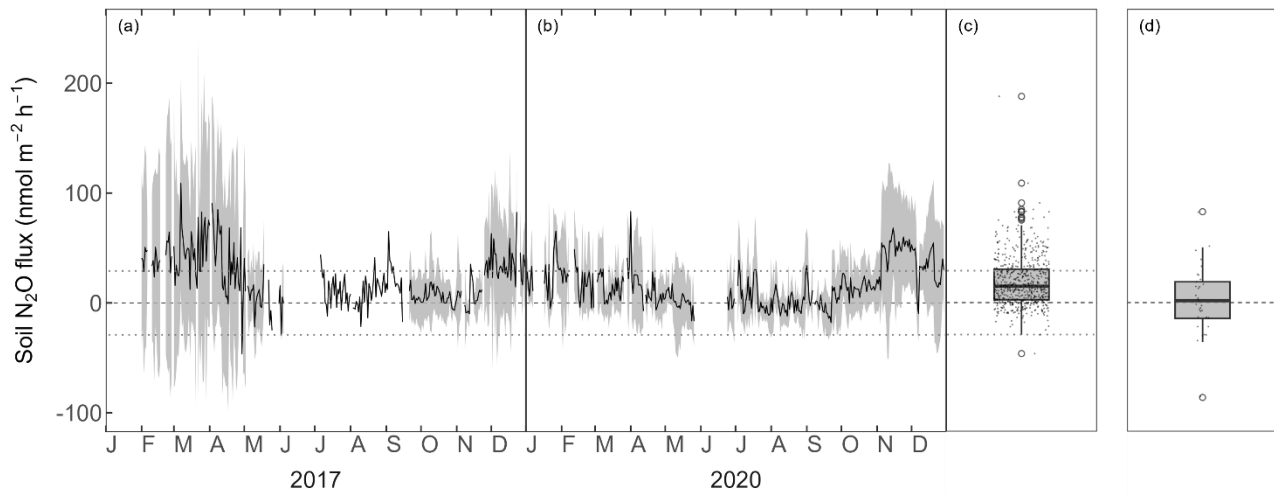


Fig. 1: Daily mean a) air temperature and soil temperature at 5 cm depth, b) water-filled pore space at 5 cm depth (left axis) and daily sum of precipitation (right axis), c) snow depth, and daily mean forest-floor d) CO_2 -respiration fluxes (not gap-filled), and e) CH_4 fluxes (not gap-filled), for the years 2017, 2020, 2021, and 2022. Please note the gap in measurements between 2017 and 2020. Black lines show means over four chambers, grey bands show standard deviations among four chambers. All data shown were quality-checked as described in the main text.

The forest floor N_2O fluxes ranged between -100 – $200 \text{ nmol m}^{-2} \text{ h}^{-1}$ but were mostly between 0 and $30 \text{ nmol m}^{-2} \text{ h}^{-1}$, with a mean over both years of $18.9 \pm 58.6 \text{ nmol m}^{-2} \text{ h}^{-1}$ (measured with automatic chambers and laser spectrometer; Fig. 2a, b, c). Winter fluxes (November to April) were generally higher and showed higher variability compared to the rest of the year. N_2O fluxes were within the calculated flux detection limit ($29.1 \text{ nmol N}_2\text{O m}^{-2} \text{ h}^{-1}$) over a large part of the measurement period. N_2O fluxes measured manually with eight static chambers in October 2023 were low (mean \pm SD = $2.9 \pm 31.1 \text{ nmol m}^{-2} \text{ h}^{-1}$).

325 Fig. 2d) and agreed very well with the fluxes measured using the automatic chambers (mean in October: 10.2 ± 14.7 nmol m⁻² h⁻¹). Both chamber measurements showed occasional N₂O uptake.



330 Fig. 2: Forest-floor N₂O fluxes (nmol m⁻² h⁻¹) for the years a) 2017 and b) 2020. Black lines show means over four chambers, grey bands show standard deviations among four chambers. Boxplots show distribution of c) mean N₂O fluxes from four automatic chambers, and d) N₂O fluxes from static chamber measurements. The dotted lines depict the minimum flux (29.1 nmol N₂O m⁻² h⁻¹) which could be detected by the Dual Quantum Cascade Laser spectrometer.

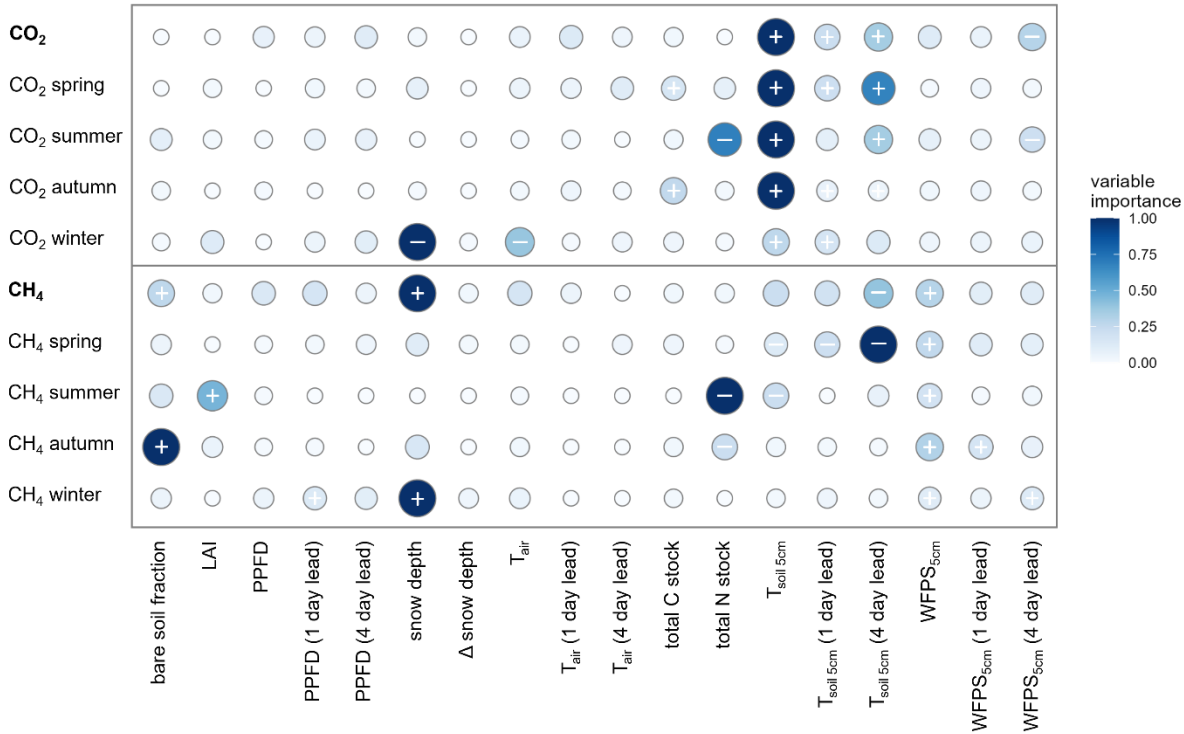
3.2 Driver analyses with random forest models

The RF models captured the temporal dynamics and absolute magnitudes of the observed forest-floor CO₂-respiration and CH₄ fluxes very well, with R² values of 0.95 and 0.87, respectively (relationships of observed vs. predicted fluxes from test datasets)₂ and RSME of 0.32 μmol m⁻² s⁻¹ and 0.27 nmol m⁻² s⁻¹, respectively (Fig. A.25). ~~Also, the~~ The seasonal RF models for forest-floor CO₂-respiration fluxes yielded high R² values of 0.94, 0.73, 0.90 and 0.63 for spring, summer, autumn and winter, respectively (Tab. A.34). Similarly, forest-floor CH₄ fluxes during spring, summer, autumn and winter were predicted well, with R² values of 0.80, 0.76, 0.72 and 0.73, respectively. Thus, the RF model performance was very good, also when shorter time periods were considered.

340 Forest-floor CO₂-respiration fluxes combined for all four years and seasons were predominantly driven by T_{soil} at 5 cm depth: T_{soil} at the time of the flux measurements was the most important driver, but also T_{soil} with a four-day (second most important) and with a one-day lead were relevant (Fig. 2 Fig. 3). Furthermore, WFPS at 5 cm with a four-day lead played an important role. As expected, higher T_{soil} lead to higher CO₂-emissionsrespiration, while higher WFPS reduced CO₂-emissionsforest-floor respiration. ~~No emissions of d~~ Drivers enhancing canopy photosynthesis, i.e., LAI or PPFD, ~~were observed~~ did not play any
345 role for forest-floor respiration. Separating ~~the~~ forest-floor CO₂-respiration fluxes into seasonal fluxes resulted in a clear

350

distinction of drivers in winter compared to the other seasons (Fig. 2Fig. 3). Winter CO_2 -respiration fluxes were mainly driven by snow depth (most important driver), leading to; higher snow depth leading to lower CO_2 -respiration fluxes with higher snow depths, while T_{soil} played a smaller role. As for the overall fluxes, summer forest-floor CO_2 -respiration fluxes were mainly driven by T_{soil} , increasing with T_{soil} , but also total N stocks were highly relevant in summer, with (higher total N stock leading to lower CO_2 -respiration fluxes), much in contrast to the fluxes during spring and fall (Fig. 2Fig. 3).



355

Fig. 2Fig. 3: Relative variable importance (rescaled to 0–1) according to the random forest driver analysis for CO_2 -forest-floor respiration (top; CO_2) and CH_4 (bottom) fluxes (not gap-filled; shown for the entire year, and per season). The direction of the effect of each predictor variable on the fluxes is shown by + (positive correlation) and - (negative correlation) signs, i.e., + indicates increased CO_2 -emissionsforest-floor respiration or decreased CH_4 uptake (i.e., increased CH_4 emissions). Signs are given for the four most important predictors which was were investigated using partial dependence plots. See Materials and Methods for variable abbreviations.

360

The RF analysis showed that forest-floor CH_4 fluxes combined for all four years and seasons were mainly driven by the snow depth, with (higher snow depths leading to more positive CH_4 fluxes and thus less CH_4 uptake; (Fig. 2Fig. 3). Furthermore, the four-day lead of T_{soil} at 5 cm impacted the fluxes negatively, leading to increased CH_4 uptake, while WFPS at 5 cm; and the bare soil fraction inside the chamber lead to strongly decreased CH_4 uptakeimpacted the fluxes. We found that the drivers

of the forest-floor CH₄ fluxes changed profoundly among seasons. Spring CH₄ fluxes were mainly temperature-driven (higher temperatures leading to more CH₄ uptake). In summer, forest-floor CH₄ fluxes were mainly driven by total N stocks (higher N stocks leading to more negative CH₄ fluxes and thus higher uptake) and by LAI (higher LAI leading to more positive CH₄ fluxes and thus lower uptake), reflecting spatial variability among chambers. In addition, CH₄ fluxes were influenced by an interaction of several drivers such as T_{soil} (higher T_{soil} leading to higher uptake) and WFPS (higher WFPS leading to lower uptake). For autumn CH₄ fluxes, bare soil fraction was the most important driver (more bare soil – and thus smaller moss cover (Tab. A.24) – leading to more positive CH₄ fluxes and thus less CH₄ uptake), but also WFPS played an important role. Winter CH₄ fluxes responded mainly to snow depth, with (higher snow depth leading to less CH₄ uptake; (Fig. 2 Fig. 3). Closer investigation of the relationship between the two most important drivers (snow depth and the four-day lead of T_{soil}) with daily CH₄ uptake over the entire year revealed that the temperature dependence of the CH₄ fluxes disappeared when snow was present (Fig. 4a). We found a significant logarithmic relationship between CH₄ uptake and snow depths, showing a decrease in CH₄ uptake with increasing snow depth (Fig. 4b). Additionally, observations of CH₄ release were mainly attributed to snow covered periods (85 % of positive CH₄ fluxes). Furthermore, the Spearman correlation coefficient between the CH₄ fluxes in the months October to May and snow depth was high with $r = 0.59$.

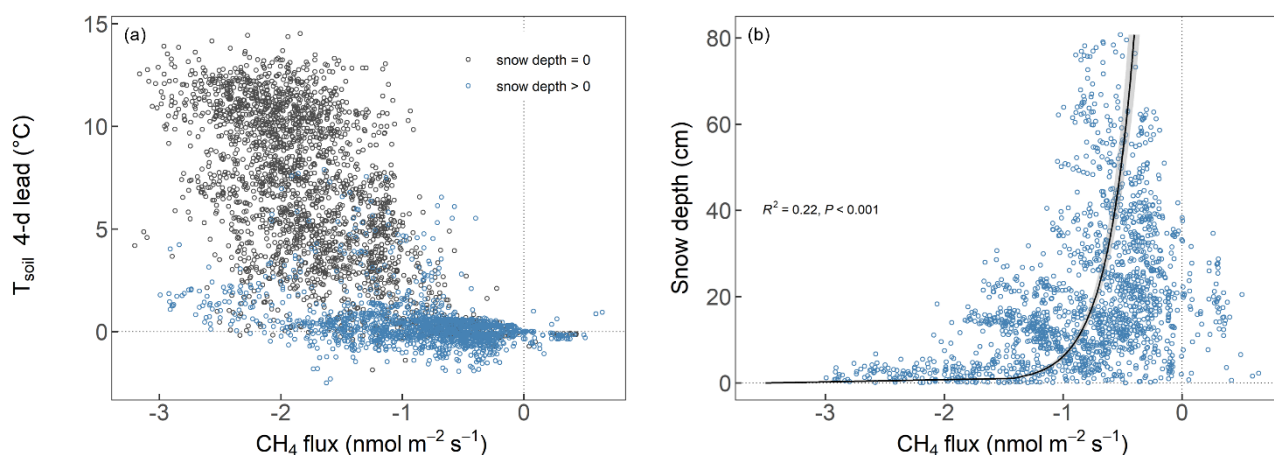


Fig. 4: Relationship between forest-floor CH₄ fluxes (nmol m⁻² s⁻¹, daily means per chamber) and a) 4-day lead of soil temperature at 5 cm depth (°C) and b) snow depth (cm) with the black line showing the fitted logarithmic curve.

3.3 Forest-floor CO₂ and CH₄ and GHG budgets

The forest floor of this subalpine spruce forest was a net-source of CO₂ and a net sink of CH₄ for all years of the study (averaged over all four chambers; Tab. 31). Mean annual forest-floor CO₂-respiration and CH₄ budgets were 2.336 ± 0.200 kg CO₂ m⁻² yr⁻¹ and -0.71 ± 0.06 g CH₄ m⁻² yr⁻¹, respectively. The annual forest-floor respiration CO₂-budgets were mainly determined by

summer and early autumn fluxes (i.e., June to September). The interannual variability (SD) of forest-floor respiration CO₂ budgets was approx. 0.200 kg CO₂ m⁻² yr⁻¹ (8.6 %) during the four years of the study, with 2017 and 2021 showing smaller and 2022 the highest emissions. The annual forest-floor respiration CO₂-budgets calculated with the Q₁₀ modeled data (2.422±0.21 kg CO₂ m⁻² yr⁻¹; Tab. 31, Fig. A.4) agreed well with the forest-floor respiration CO₂-budgets based on the gap-filled fluxes using RF, also showing highest fluxes in 2022. A similar interannual variability (SD) as for the respiration CO₂ budgets was found for the CH₄ budgets, with 8.5 % (0.06 g CH₄ m⁻² yr⁻¹). Comparing the magnitudes of the forest-floor respiration CO₂ and CH₄ budgets (in CO₂-eq) clearly showed that the respiration CO₂-budget determined the forest-floor GHG C budget of the spruce forest, since the CH₄ uptake (-19.1±1.8 g CO₂-eq m⁻² yr⁻¹) was about two orders of magnitude smaller than the CO₂ emissions/respiration fluxes (2336±200 g CO₂-eq m⁻² yr⁻¹). We did not develop an RF model for N₂O fluxes and did thus not calculate a forest-floor N₂O budget based on gap-filled fluxes. However, using the mean N₂O flux measured with the automatic chambers over two years (18.9 nmol m⁻² h⁻¹), we estimated the annual forest-floor N₂O budget to be 0.007±0.025 g N₂O m⁻² yr⁻¹. Using the 100-year global warming potential of N₂O of 273 (IPCC, 2021) resulted in an annual forest-floor N₂O budget of 1.99 g CO₂-eq m⁻² yr⁻¹, representing 0.09 % of the annual forest-floor GHG budget (i.e., all three gases).

Tab. 31: Mean annual budgets (±standard deviation (SD) over four chambers) of CO₂ forest-floor respiration and CH₄ forest-floor fluxes (using gap-filled data). The Q₁₀ budget was calculated with Eq. 3 (Q₁₀ and R_{ref} estimates were 4.8 and 3.16, respectively; overall R² was 0.86).

Year	<u>CO₂ Forest-floor respiration</u> budget			<u>Forest-floor CH₄</u> budget			Net <u>GHG-C</u> budget based on RF (g CO ₂ -eq m ⁻² yr ⁻¹)
	based on RF (g CO ₂ m ⁻² yr ⁻¹)	based on RF (g C m ⁻² yr ⁻¹)	based on Q ₁₀ budget (g CO ₂ m ⁻² yr ⁻¹)	based on RF (g CO ₂ -eq m ⁻² yr ⁻¹)	based on RF (g C m ⁻² yr ⁻¹)	(g CH ₄ m ⁻² yr ⁻¹)	
2017	2139±334	584±91	2407±28	-17.1±3.6	-0.47±0.10	-0.63±0.13	2122±334
2020	2338±324	638±89	2390±54	-18.7±3.3	-0.52±0.09	-0.69±0.12	2319±324
2021	2138±275	584±75	2204±40	-18.3±2.7	-0.51±0.08	-0.68±0.10	2120±275
2022	2730±589	745±161	2687±40	-22.2±4.4	-0.62±0.12	-0.82±0.16	2708±579
Overall	2336±200	638±55	2422±21	-19.1±1.8	-0.53±0.05	-0.71±0.06	2317±200

The year 2022 can be considered an exceptional year, both in terms of annual forest-floor respiration CO₂- and CH₄ fluxes (Tab. 13), but also in terms of temporal development (Fig. 3 Fig. 5a). For CO₂, there were not only higher emission/respiration rates in summer, but also a faster increase in CO₂ emission/respiration rates already in mid-April and sustained higher emissions rates until later in the year (Fig. 3 Fig. 5a). The exceptionally high CO₂ forest-floor respiration fluxes (2022 forest-floor respiration budget falls outside the 95% confidence interval = ±1.96SD, i.e., for the forest-floor respiration budget: ± 392 g CO₂ m⁻² yr⁻¹) coincided with the higher-than-usual T_{soil} (annual mean T_{soil} of 2022 falls outside the 95% confidence interval) which was the main driver of spring, summer, and autumn forest-floor respiration CO₂-fluxes. For CH₄, we observed a considerably higher annual CH₄ uptake in 2022 compared to other years (Tab. 13), mainly due to higher uptake rates in summer as well as still high uptake rates in autumn and early winter (Fig. 3 Fig. 5b). Apart from higher T_{soil} driving the higher summer

CH₄ uptake, this was mainly connected to comparably low soil moisture in autumn 2022 and the ~~exceptionally~~ low snow amount depths in November and December 2022.

415

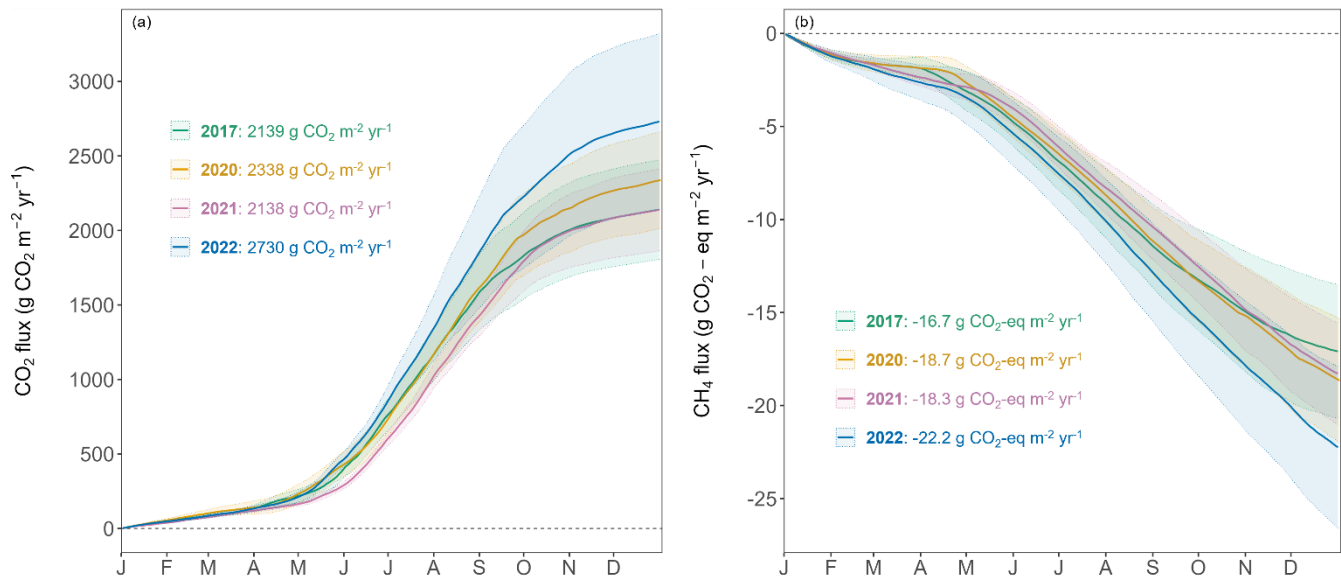


Fig. 3 Fig. 5: Cumulative ~~forest-floor~~ (a) ~~respiration~~ CO₂ (g CO₂ m⁻² yr⁻¹) and (b) CH₄ (g CO₂-eq m⁻² yr⁻¹) ~~forest-floor~~ fluxes over four years. Lines show means of all four chambers; colored bands represent standard deviations among four chambers.

4 Discussion

420 4.1 Interannual variability in forest-floor GHG fluxes

Over the four-year measurement period (2017 and 2020–2022), we ~~acquired~~ ~~collected~~ high-resolution, ~~reliable~~ forest-floor GHG flux ~~data measurements~~ for four ~~very~~ distinct years allowing comprehensive year-round analyses. Notably, 2022 emerged as the warmest year ever recorded at the Davos site ~~so far~~, coinciding with remarkably low precipitation ~~and WFPS~~ levels. ~~Despite these counteracting environmental conditions,~~ ~~The~~ forest-floor ~~CO₂ emissions~~ ~~respiration~~ in 2022 exceeded ~~those in~~ the other three years by approximately 20 %. Concurrently, we observed the highest forest-floor CH₄ uptake in 2022. ~~It is well known that temperature is a major driver for any respiratory process~~ (Davidson et al., 2006; Amthor, 2000). ~~Also our RF driver analysis revealed that soil temperature was the main driver for forest-floor respiration fluxes, while no soil water limitation existed at this high elevation forest site during the study period~~. Anjileli et al. (2021) reported that ~~at multiple sites across the contiguous United States~~ even during extreme heat events, soil respiration increased by approximately 25 % compared to average conditions, emphasizing the dominating influence of temperature on ~~CO₂ emissions~~ ~~respiration~~ also under extreme dry conditions ~~for those sites~~. Additionally, Borken et al. (2006) indicated that droughts can enhance the soil CH₄ sink in temperate forests. In contrast, the year 2021 was the coldest year among the four years we investigated, with an annual mean T_{air} of 3.9

425

430

°C₂ mainly driven by below-average spring temperatures. This was reflected clearly in the GHG fluxes with below-average ~~CO₂-emissionsforest-floor respiration rates~~ (approximately 30 % lower compared to the four-year mean) and below-average
435 CH₄ uptake in spring 2021 (approximately 20 % lower compared to the four-year mean). Moreover, 2021 was an exceptional year in terms of snow ~~amount-depth, a relevant driver identified in this study~~ (snow depth in winter and spring exceeded the four-year average by 87 % and 145 %, respectively), ~~relevant drivers identified in this study~~.

While the year 2020 was also characterized by ~~a~~ warm weather, its summer temperatures were less extreme than ~~those~~ in 2022. Our findings revealed that the ~~CO₂-emissionsforest-floor respiration~~ in 2020 did not reach the levels observed in 2022,
440 supporting our driver analyses, clearly indicating that the exceptionally high summer temperatures experienced in 2022 were the primary driving force behind the 2022 annual ~~CO₂-emissionsforest-floor respiration fluxes~~. The RF models for 2022 resulted in slightly lower forest-floor ~~CO₂ fluxes-respiration~~ than measured, suggesting that no overfitting had occurred (Fig. A.36, A.47). Moreover, these results highlighted the critical role played by extreme summer temperatures in shaping the C dynamics of this subalpine spruce ecosystem and underscored the significance of understanding their implications for future
445 C budgets, potentially reducing the overall C sink ~~behavior-capacity~~ observed so far in this forest (Zielis et al., 2014).

~~We measured very low forest-floor N₂O fluxes which agreed well between the two measurement techniques used (automatic chambers and laser spectroscopy vs. static chambers and gas chromatography). Due to soil aeration and soil moisture conditions at our site, we assumed that nitrification and not denitrification was the main process responsible for the N₂O emissions measured (Papen and Butterbach-Bahl, 1999; Butterbach-Bahl et al., 2013). At our site, N supply to plants and
450 microorganisms is limited. Foliage N concentrations indicate N limitation for spruce (foliar N concentration are about 1% in 0- and 1-yr-old needles as opposed to the optimum range of N content in needles between 1.5 and 2.3 %; (Thimonier et al., 2010; Ingestad, 1959). Furthermore, N concentrations in the soil are low (1.4% in the organic layer, 0.4% in 10-20 cm depth; Jörg, 2008), as well as N deposition (about 10 kg N ha⁻¹ yr⁻¹; (Thimonier et al., 2019; Gharun et al., 2021). Thus, our site is rather low in N, which could be used for microbial transformations like nitrification, competing with plant uptake (Schulze,
455 2000), therefore, low soil N₂O fluxes were to be expected. The observations of occasional low N₂O uptake measured with static and automatic chambers are in line with (Goldberg and Gebauer, (2009) who observed N₂O uptake in a German spruce forest. Microbial processes in forest soils can contribute to both uptake and release of N₂O, depending on the prevailing environmental conditions such as oxygen availability, soil moisture and microbial communities. Under anaerobic conditions, denitrification contributes to N₂O release, while under aerobic conditions, N₂O reduction to N₂ can dominate over N₂O
460 production, which results in observations of net N₂O uptake by soils (Wen et al., 2017).~~

4.2 Drivers of forest-floor GHG fluxes

Forest-floor GHG fluxes were shown to have very distinct drivers across the different seasons. Consistent with our expectations, soil temperature predominantly controlled forest-floor ~~respiration~~ CO₂-fluxes, thereby influencing the ~~annual~~
465 ~~respiration~~ CO₂-budget at annual as well as seasonal scales (except winter season). In contrast, no effects of drivers known to

enhance canopy photosynthesis (i.e., LAI, PPFD) and thus below-ground allocation and soil respiration (Högberg et al., 2001) were observed on the forest-floor ~~respiration~~ CO_2 -fluxes for any time in this spruce forest, suggesting a strong direct control of environmental factors and only a weak or even lacking indirect control of canopy biology or structure. Drivers of forest-floor CH_4 fluxes were much more variable compared to those ~~for~~ of forest-floor respiration CO_2 -fluxes, with winter CH_4 fluxes being affected by the same driver (snow depth) as the annual fluxes. ~~In addition, CH_4 fluxes responded most strongly to WFPS in autumn.~~ These findings that snow depth and WFPS (in autumn) were important drivers of forest-floor CH_4 fluxes supported the hypothesis proposed by Borken et al. (2006), which-who emphasized the role of factors influencing the diffusion rates of atmospheric CH_4 into the soil, such as ~~soil water content~~ SWC and snow cover, in determining CH_4 uptake in forest soils. Notably, previous studies have-had also reported a close relationship between CH_4 fluxes and seasonal changes in soil moisture (Ni and Groffman, 2018; Ueyama et al., 2015). However, our results indicated that in spring and summer, T_{soil} rather than WFPS played a more important role in driving forest-floor CH_4 uptake. Additionally, we identified a notable influence of soil N on summer CH_4 fluxes, with higher N stocks, and thus most likely higher N mineralization during the summer months, corresponding to enhanced CH_4 uptake. This aligneds with previous findings in forest ecosystems, where soil mineral N hads been shown to stimulate CH_4 oxidation (Goldman et al., 1995; Martinson et al., 2021). Moreover, we found a positive correlation between bare soil fraction and forest-floor CH_4 uptake, i.e., less-more bare soil and thus higher-lower moss cover leading to higher-lower forest-floor CH_4 uptake. This is in line with ~~the~~ findings that *Sphagnum* mosses can promote CH_4 oxidation (Basiliko et al., 2004). Also, for forest-floor CH_4 fluxes, hardly any effect of tree canopy biology was detected (except for summer). Thus, a strong direct control of environmental factors on both GHG-forest-floor respiration and CH_4 fluxes was observed, increasing the vulnerability of the forest C sink with future climate change (IPCC, 2021).

485 4.3 Forest-floor C and GHG budgets

The overall forest-floor GHG-C budget (i.e., CO_2 and CH_4) showed a total emission of $2317 \pm 200 \text{ g CO}_2\text{-eq m}^{-2} \text{ yr}^{-1}$, dominated by the annual forest-floor respiration CO_2 -budget ($2336.34 \pm 0.200 \text{ kg CO}_2 \text{ m}^{-2} \text{ yr}^{-1}$), which was within the range of studies conducted in temperate, subalpine or boreal forests which we considered comparable to our site ($1.070\text{--}2.906 \text{ kg CO}_2 \text{ m}^{-2} \text{ yr}^{-1}$; Gaumont-Guay et al., 2014; Groffman et al., 2006; Schindlbacher et al., 2007, 2014; Wang et al., 2013; Xu et al., 2015). Also our estimate of annual CH_4 budget at the site ($-0.71 \pm 0.06 \text{ g CH}_4 \text{ m}^{-2} \text{ yr}^{-1}$) fell within the range of -1.6 to $-0.18 \text{ g CH}_4 \text{ m}^{-2} \text{ yr}^{-1}$ observed in other forest studies (Borken et al., 2006; Luo et al., 2013; Ueyama et al., 2015; Yu et al., 2017), offsetting a mere 0.8 % of the forest-floor respiration CO_2 -emissions. Our estimate of the annual N_2O budget of $0.0073 \text{ g N}_2\text{O m}^{-2} \text{ yr}^{-1}$ agreed well with previous studies (Rütting et al., 2021; Ullah et al., 2009). For instance, a study conducted in a boreal spruce forest with low N deposition rates (about $5 \text{ kg N ha}^{-1} \text{ yr}^{-1}$) reported very low mean N_2O fluxes of around $0.0077 \text{ g N}_2\text{O m}^{-2} \text{ yr}^{-1}$ (Rütting et al., 2021). Winter fluxes contributed a large fraction to the overall CH_4 budget (14.4–18.4 %), but played a less important role for the forest-floor respiration CO_2 -budget (6.0–7.3 %), similar to the CO_2 contribution in other mid latitude and temperate ecosystems (5.5–8.9 %; Gao et al., 2018; Wang et al., 2013) but smaller than some high latitude and other subalpine ecosystems (12–20 %; Kim et al., 2017; Schindlbacher et al., 2007; Xu et al., 2015).

To date, only a few studies have examined soil or forest-floor GHG fluxes in subalpine, temperate, or boreal forests measuring CO₂, CH₄ and N₂O fluxes in parallel (Tab. 24). Tab. 2 includes studies examining fluxes from both the forest floor (soil and ground vegetation) and the soil. However, their comparability is constrained as forest-floor flux measurements encompass both soil respiration (including heterotrophic and root respiration) and autotrophic respiration from forest-floor plants, whereas soil flux measurements specifically capture soil respiration (Barba et al., 2018). It is noteworthy that the integration of year-round and temporally highly resolved measurements remains rather uncommon; to our knowledge, only two other studies with year-round measurements of CO₂, CH₄ and N₂O exist apart from the current study (Luo et al., 2011; Pilegaard et al., 2003). On the one hand, previous studies frequently measured fluxes for only a limited period of the year, often excluding the dormant season. On the other hand, many of the studies adopted a weekly to monthly measurement frequency, potentially missing the full range of, consequently being unable to detect any short-term hot moments, and thus potentially underestimating the flux magnitudes. If year-round measurements of forest-floor CO₂ fluxes/respiration are not feasible, using Q₁₀ models might be a viable option, as long as the annual temperature range is being well covered, as seen in the agreement between our budget based on gap-filled continuous measurements and the Q₁₀ budget. However, although T_{soil} was identified as the primary driver of CO₂ emissions/forest-floor respiration, it was not the only one driver. We argue that Q₁₀ models are not able to capture extreme respiration fluxes which might be caused by more drivers than temperature alone. Many studies have shown that Q₁₀ models do not reproduce measured fluxes well when additional drivers impact the fluxes, for instance when soil moisture, frost, or carbohydrate limitations come into play (e.g., Ruehr et al., 2010; Reichstein et al., 2013; Mitra et al., 2019). In contrast, our high-resolution dataset coupled with machine learning offered a more comprehensive approach, which included multiple environmental variables and at the same time was able to consider chamber-specific characteristics, and thus was able to capture the extreme fluxes we observed in summer 2022. Thus, we think that the reliability of the RF budget is higher than that of the Q₁₀ budget. Thus, neglecting other potential drivers might reduce the reliability and increase the uncertainty of any (modeled) annual CO₂ budget. Moreover, identifying important drivers for GHG fluxes is the more reliable, the longer and thus typically the more frequent measurements were done. Additionally, to effectively capture the dynamic nature of soil and/or forest-floor GHG fluxes, it is essential to use automatic chambers with high temporal resolution, preferentially opaque to exclusively quantify respiration. Therefore, we recommend continuous, year-round measurements to reliably estimate annual forest-floor C and GHG budgets, particularly when large seasonal variability of potential drivers is expected, or when the duration of the active period, i.e., start and end of the snow-free period, is highly variable like in high elevation or high latitude ecosystems. Particularly with the anticipated impacts of future climate change (IPCC, 2021), duration of growing periods will change, and winter fluxes (or the lack thereof) will gain increasing importance (Xie et al., 2017).

Tab. 42: Previously published studies investigating forest-floor or soil CO₂, CH₄ and N₂O fluxes in parallel in temperate, subalpine, or boreal forests using automatic or static chambers. n.a. = not available.

Chamber method	Location	Forest type	Years	Duration	No.# chambers	Frequency	Veg. in chambers	CO ₂ flux rates ($\mu\text{g CO}_2 \text{ m}^{-2} \text{ s}^{-1}$)	CH ₄ flux rates ($\text{ng CH}_4 \text{ m}^{-2} \text{ s}^{-1}$)	N ₂ O flux rates ($\text{ng N}_2\text{O m}^{-2} \text{ s}^{-1}$)	Reference
Automatic	46.82° N 9.86° E	Subalpine (spruce)	2017, 2020–2022	Year-round	4	3 h	Yes	<u>74.1±6.3</u>	<u>-22.5±1.9</u>	<u>0.2±0.8</u>	This study
Automatic	39.09° N 75.44° W	Temperate (mixed)	2017	Apr–Jul	3	1 h	No	<u>362.6±24.2</u>	<u>-10.6±1.0</u>	<u>-2.0±0.5</u>	Barba et al., 2019
Static	43.23° N 3.20° W	Radiata pine, Douglas fir, beech	2010–2011	Year-round	6	Biweekly	Yes	<u>14.7±1.6</u>	<u>0.8±0.1</u>	<u>1.3±0.4</u>	Barrena et al., 2013
Static	37.07° N 119.19° W	Montane mixed-conifer (Mediterranean-type climate)	2010–2012	Snow free period	24	Weekly–monthly	n.a.	<u>51.7–63.3</u>	<u>-9.6–4.8</u>	<u>-0.3–1.7</u>	Blankinship et al., 2018
Static	35.66° S 148.15° E	Temperate (eucalypt)	2006	2 weeks in Nov	10	4 h	No	<u>90.4±1.9</u>	<u>-19.2±0.4</u>	<u>1.4±0.04</u>	Fest et al., 2009
Static	43.93° N 71.75° W	Northern hardwood (beech, maple, birch)	1998–2000	Year-round	8	Weekly–monthly	n.a.	<u>26.7–46.5</u>	<u>-20.0–7.9</u>	<u>2.0–7.0</u>	Groffman et al., 2006
Static	42.40° N 128.10° E	Broad-leaved Korean pine mixed	2019	Mar–Oct	8	Twice a week–twice a month	n.a.	<u>241.0±114.9</u>	<u>-35.9±12.5</u>	<u>9.7±6.2</u>	Guo et al., 2020
Static	48.09° N 16.01° E	Temperate (beech)	1997	Apr–Nov	8	Biweekly	Yes	<u>53.0–57.8</u>	<u>-5.6–3.2</u>	<u>11.9–30.5</u>	Hahn et al., 2000
Static	43.83° N 74.87° W	Temperate (mixed)	2008	May–Jul	15	Biweekly	Yes	<u>10.2–101.8</u>	<u>-16.7–42.1</u>	<u>-1.2–2.8</u>	Hopfensperger et al., 2009
Static	47.03° N 8.72° E	subalpine (spruce)	2007–2012	Year-round	10	Every 3 weeks	Yes	<u>48.8</u>	<u>-8.0–13.4</u>	<u>-1.2–2.9</u>	Krause et al., 2013
Automatic (CO ₂), static (CH ₄ , N ₂ O)	48.50° N 11.17° E	Temperate (spruce)	1994–1997, 2000–2010	Year-round	5	1 h (CO ₂), 2 h (CH ₄ , N ₂ O)	n.a.	<u>81.3–106.9</u>	<u>-14.8–3.8</u>	<u>1.0–14.9</u>	Luo et al., 2011
Static	46.67–47.93° N 91.75–92.52° W	Boreal-temperate (mixed)	2013	May–Oct	48	Monthly	Yes	<u>0.002–0.004</u>	<u>-0.0014–-0.0003</u>	<u>-10.3–10.3</u>	Martins et al., 2017
Static	33.30–33.47° N 108.35–108.65° E	Temperate–cold temperate (deciduous broad-leaved & coniferous)	2012–2014	Year-round	60	Weekly–monthly	Yes	<u>44.4–86.9</u>	<u>-24.0–3.8</u>	<u>5.9–11.2</u>	Pang et al., 2023

Automatic (CO ₂), static (CH ₄ , N ₂ O)	55.48° N 11.63° E	Temperate (beech)	1998–1999, 2001	Year-round	5 (CO ₂), 6 (CH ₄ , N ₂ O)	2 h (CO ₂), biweekly (CH ₄ , N ₂ O)	<u>Yes</u>	<u>n.a.</u>	<u>n.a.</u>	<u>n.a.</u>	Pilegaard et al., 2003
Automatic	45.20° N 68.74° W	Sub-boreal (spruce, hemlock)	2013–2016	May–Nov	3-5	30 min	<u>n.a.</u>	<u>n.a.</u>	<u>n.a.</u>	<u>n.a.</u>	Richardson et al., 2019
Concentration profiles	41.33° N 106.33° W	Subalpine (spruce, fir)	1991–1992	Mar–May	2	Daily–biweekly	<u>Yes</u>	<u>18.3–31.6</u>	<u>-0.0029–-0.0004</u>	<u>0.0003–0.0004</u>	Sommerfeld et al., 1993
Static	49.26–52.20° N 74.03–76.07° W	Boreal (black spruce, jack pine, aspen, alder)	2007	May–Oct	48	Monthly	<u>Yes</u>	<u>34.4–64.0</u>	<u>-6.7–1.6</u>	<u>0.4–0.8</u>	Ullah et al., 2009
Static	57.13° N 14.75° E	Cold temperate (coniferous)	1999–2002	Year-round	30	Weekly–biweekly	<u>Yes</u>	<u>28.5–60.2</u>	<u>0.0–50.7</u>	<u>1.0–2.9</u>	Von Arnold et al., 2005
Static	53.28–53.50° N 122.10–122.45° E	Cold temperate continental monsoon	2016–2018	Year-round	9	Weekly–monthly	<u>Yes</u>	<u>2.2–180.8</u>	<u>-15.9–9.0</u>	<u>-1.1–8.6</u>	Wu et al., 2019

5 Conclusions

535 ~~We measured year-round~~ Forest-floor GHG fluxes, ~~measured~~ during multiple years with ~~four~~ large opaque automatic chambers, ~~were mainly driven by environmental factors, with only limited impacts of tree biology or structure, and were able to identify~~
540 ~~their most important drivers. Particularly, in the~~ light of climate change-induced variations in the onset of the active growing season, growing season length, and winter conditions, we recommend to spatially expand the deployment of such chambers at research stations capable of year-round measurements, including ~~the~~ periods with snow cover. ~~Since our forest study site was~~
~~very low in N supply and thus N₂O fluxes were very low, it remains to be seen how large annual N₂O emissions are from other~~
545 ~~forest sites with higher N supply and what drivers are most relevant.~~ As temperatures will continue to rise due to climate change, and warm and dry conditions, such as in the ~~previous-recent~~ summers, are projected to become more frequent and more severe, we expect an increase in forest-floor ~~GHG emissions~~respiration at the Davos ~~spruce forest~~ and similar subalpine or high latitude ~~sites~~ecosystems. ~~Similarly, a~~Anticipated milder winters with reduced snowfall, resulting in shorter snow cover duration and lower average snow depth, will likely contribute to enhanced forest-floor ~~CO₂ emissions~~respiration and increased forest-floor CH₄ uptake in the future. Since ~~CO₂ emissions~~respiratory CO₂ losses are typically much larger than the CH₄ uptake,
545 ~~such~~ as at our site, we expect the forest floor to become a more substantial ~~GHG-C~~ source in the future, potentially reducing the overall C sink ~~capacity~~ of this type of forest.

Data availability. The data used in this study will be made publicly available from the ETH Research Collection (<https://doi.org/10.3929/ethz-b-000619728>, preliminary link).

550 *Author contributions.* NB designed the study; PM, LK and SB conducted the field work; SB and LK processed the data; LK performed the data analyses, developed the models, and wrote the manuscript draft; SB, MG, PM, IF and NB commented on the manuscript and contributed substantially to discussions and revisions.

Competing interests. The authors declare that they have no conflict of interest.

555 *Acknowledgements.* The authors thank our colleagues Lutz Merbold, Matti Barthel, Lukas Hörtnagl, Thomas Baur, Werner Eugster and Liliana Scapucci for their assistance in designing and setting up the chambers, conducting fieldwork, and providing helpful inputs during the flux processing and data interpretation. Their contributions have greatly contributed to the progress of this study.

Financial support. This research has been supported by the Swiss National Science Foundation (SNSF), in the projects ICOS-CH Phase 1, 2, 3 (Grant-N° 20FI21_148992, 20FI20_173691, 20FI20_198227) and COCO (Grant-N° 200021_197357).

Tab. A.1: 10th percentiles of R² values from linear regressions used for flux calculations per gas, given separately for each chamber (FF1 to FF4) and growing and dormant periods. Percentiles were applied as quality thresholds.

<u>Gas</u>	<u>Period</u>	<u>FF1</u>	<u>FF2</u>	<u>FF3</u>	<u>FF4</u>
<u>CO₂</u>	<u>growing period</u>	<u>0.97</u>	<u>0.98</u>	<u>0.98</u>	<u>0.99</u>
	<u>dormant period</u>	<u>0.35</u>	<u>0.48</u>	<u>0.47</u>	<u>0.68</u>
<u>CH₄</u>	<u>growing period</u>	<u>0.92</u>	<u>0.96</u>	<u>0.92</u>	<u>0.93</u>
	<u>dormant period</u>	<u>0.41</u>	<u>0.26</u>	<u>0.21</u>	<u>0.61</u>

565 Tab. A.2: Site characteristics of the four chambers (FF1 to FF4). Annual means and standard deviations are shown for soil temperature (T_{soil}) and water filled pore space (WFPS) at 5 cm, mean and max snow depth, and days with snow cover. LAI, soil, and vegetation cover inside each chamber were determined in June 2022. Soil data (bulk density, pH, C and N stocks in the topsoil, i.e., litter, organic material layers, and 0–20 cm depth of mineral soil) were taken from Jörg (2008) and (Saby et al., (2023)).

<u>Site characteristics</u>	<u>FF1</u>	<u>FF2</u>	<u>FF3</u>	<u>FF4</u>	<u>Mean</u>
<u>T_{soil} at 5cm (°C)</u>					
<u>2017</u>	<u>4.44 ± 4.67</u>	<u>4.16 ± 4.84</u>	<u>4.29 ± 4.86</u>	<u>4.56 ± 4.52</u>	<u>4.36 ± 0.17</u>
<u>2020</u>	<u>4.66 ± 4.32</u>	<u>4.40 ± 4.46</u>	<u>4.46 ± 4.34</u>	<u>4.87 ± 4.15</u>	<u>4.60 ± 0.22</u>
<u>2021</u>	<u>4.18 ± 4.25</u>	<u>3.80 ± 4.48</u>	<u>3.74 ± 4.84</u>	<u>4.26 ± 4.20</u>	<u>3.99 ± 0.26</u>
<u>2022</u>	<u>5.15 ± 4.70</u>	<u>4.83 ± 4.96</u>	<u>4.70 ± 5.38</u>	<u>5.18 ± 4.61</u>	<u>4.97 ± 0.24</u>
<u>WFPS at 5 cm (%)</u>					
<u>2017</u>	<u>20.1 ± 5.09</u>	<u>17.2 ± 4.30</u>	<u>21.3 ± 6.82</u>	<u>22.5 ± 7.42</u>	<u>20.3 ± 2.27</u>
<u>2020</u>	<u>15.9 ± 2.88</u>	<u>15.5 ± 3.85</u>	<u>9.8 ± 0.69</u>	<u>23.9 ± 9.55</u>	<u>16.3 ± 5.79</u>
<u>2021</u>	<u>16.8 ± 3.88</u>	<u>14.5 ± 3.88</u>	<u>11.8 ± 4.45</u>	<u>25.0 ± 10.5</u>	<u>17.0 ± 5.70</u>
<u>2022</u>	<u>15.1 ± 4.19</u>	<u>12.7 ± 3.27</u>	<u>10.4 ± 3.56</u>	<u>21.3 ± 7.16</u>	<u>14.9 ± 4.70</u>
<u>Max snow depth (cm)</u>					
<u>2017</u>	<u>34.7</u>	<u>40.7</u>	<u>27.4</u>	<u>25.6</u>	<u>47.4 ± 24.5</u>
<u>2020</u>	<u>31.8</u>	<u>41.7</u>	<u>25.9</u>	<u>22.0</u>	<u>58.6 ± 30.0</u>
<u>2021</u>	<u>83.9</u>	<u>103.0</u>	<u>79.5</u>	<u>62.6</u>	<u>43.5 ± 25.0</u>
<u>2022</u>	<u>39.4</u>	<u>48.7</u>	<u>41.1</u>	<u>36.8</u>	<u>36.8 ± 18.3</u>
<u>Mean snow depth (cm)</u>					

<u>2017</u>	<u>5.8 ± 8.4</u>	<u>6.4 ± 9.8</u>	<u>4.5 ± 6.4</u>	<u>3.9 ± 6.2</u>	<u>5.1 ± 1.2</u>
<u>2020</u>	<u>4.3 ± 7.0</u>	<u>8.6 ± 12.1</u>	<u>4.2 ± 7.0</u>	<u>3.5 ± 6.0</u>	<u>5.2 ± 2.3</u>
<u>2021</u>	<u>17.6 ± 25.0</u>	<u>22.2 ± 29.5</u>	<u>14.6 ± 22.7</u>	<u>14.8 ± 21.0</u>	<u>17.3 ± 3.6</u>
<u>2022</u>	<u>5.1 ± 9.3</u>	<u>8.3 ± 14.1</u>	<u>6.1 ± 11.7</u>	<u>4.9 ± 9.5</u>	<u>6.1 ± 1.6</u>
<u>Days with snow cover</u>					
<u>2017</u>	<u>152</u>	<u>159</u>	<u>152</u>	<u>148</u>	<u>153 ± 5</u>
<u>2020</u>	<u>126</u>	<u>142</u>	<u>123</u>	<u>117</u>	<u>127 ± 11</u>
<u>2021</u>	<u>172</u>	<u>189</u>	<u>161</u>	<u>169</u>	<u>173 ± 12</u>
<u>2022</u>	<u>138</u>	<u>145</u>	<u>134</u>	<u>132</u>	<u>137 ± 6</u>
<u>Leaf area index (LAI)</u>	<u>2.9</u>	<u>4.2</u>	<u>3.1</u>	<u>2.9</u>	<u>3.3 ± 0.6</u>
<u>Soil cover inside chamber (%)</u>					
<u>bare soil</u>	<u>0</u>	<u>50</u>	<u>70</u>	<u>0</u>	<u>30 ± 36</u>
<u>moss</u>	<u>90</u>	<u>50</u>	<u>20</u>	<u>90</u>	<u>63 ± 34</u>
<u>grass</u>	<u>5</u>	<u>1</u>	<u>0</u>	<u>0</u>	<u>2 ± 2</u>
<u>Vaccinium</u>	<u>60</u>	<u>0</u>	<u>10</u>	<u>30</u>	<u>25 ± 26</u>
<u>Bulk density at 5 cm of mineral soil (g cm⁻³)</u>	<u>0.27</u>	<u>0.35</u>	<u>0.32</u>	<u>0.35</u>	<u>0.32 ± 0.04</u>
<u>pH</u>	<u>2.8–3.1</u>	<u>3.0–3.4</u>	<u>2.8–3.1</u>	<u>3.0–3.4</u>	
<u>C stock (t/ha)</u>	<u>93.5</u>	<u>147.7</u>	<u>135.4</u>	<u>105.8</u>	<u>120.6 ± 25.2</u>
<u>N stock (t/ha)</u>	<u>3.54</u>	<u>5.74</u>	<u>4.47</u>	<u>3.52</u>	<u>4.32 ± 1.05</u>

570



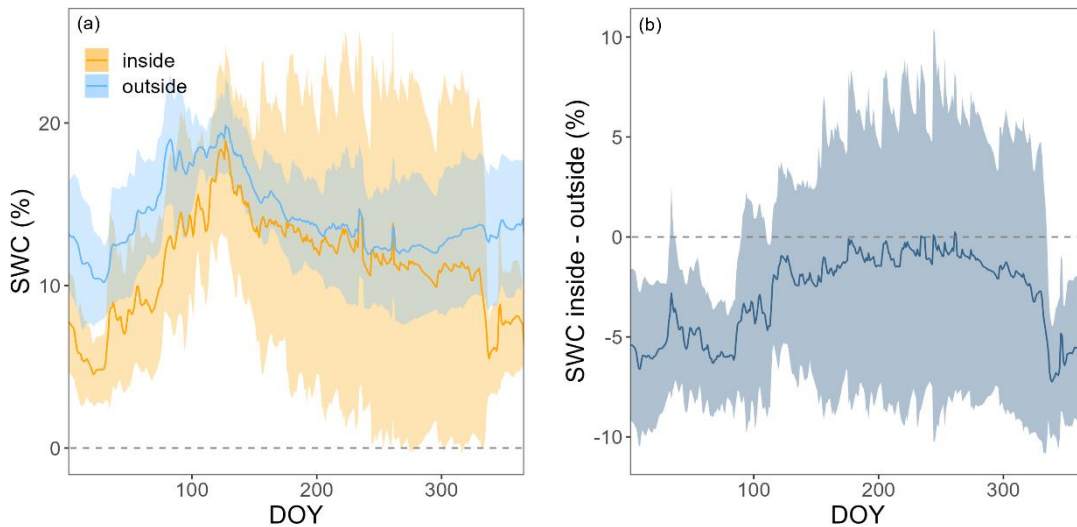
Fig. A.1: Picture of one of the automatic chambers (at location FF3).

575

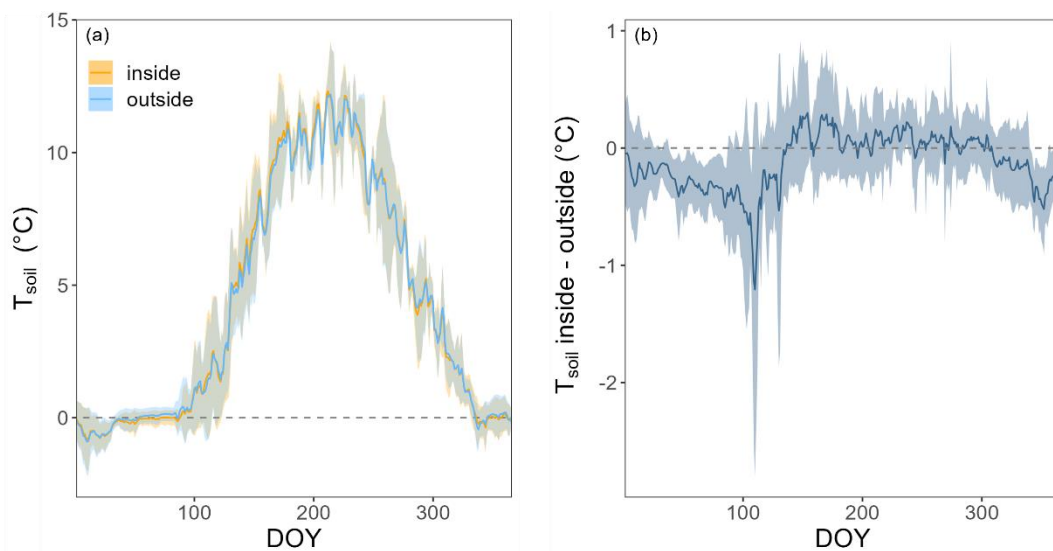
Tests for chamber biases

580 We tested for chamber effects using SWC measurements from inside and outside FF1 and FF2 over all four years (Fig. A.2). SWC was highly variable over time as well as in space (Fig. A.2a). SWC differences between inside and outside the chamber varied between +10% and -10% during the four years (Fig. A.2b). No clear trend was detectable over time. The average difference between inside and outside SWC over the four years was $-2.9 \pm 5.8\%$. No significant differences in SWC inside vs. outside the chamber were detected during most of the year (exception: during winter, on average 5% lower SWC values inside compared to outside of the chamber). We found a high agreement in the dynamics of SWC inside and outside FF1 and FF2 (R^2 values of 0.69 and 0.82, respectively). In terms of T_{soil} , we did not find any significant differences inside vs. outside the chambers over most of the year (Fig. A.3a). The differences were only significantly different from zero in the months December, February, and March when T_{soil} inside the chambers was around 0.1-0.5 °C lower than outside the chambers (Fig. A.3b). At prevailing soil temperatures of around 0 °C in these months, such a difference in T_{soil} has no effect on the magnitude of forest-floor respiration (Fig. A.4).

585



590 Fig. A.2: a) Soil water content (SWC) at 5 cm inside (orange) and outside (light blue) and b) the difference in SWC at 5 cm between inside and outside the chambers FF1 and FF2 over the course of a year. Lines show means, bands show standard deviations over all four years.



595

Fig. A.3: a) Soil temperatures (T_{soil}) at 5 cm inside (orange) and outside (light blue) and b) difference in T_{soil} at 5 cm between inside and outside of chambers (FF1 to FF4) over the course of a year. Lines show means, bands show standard deviations over three years (2017, 2020 and 2021).

600

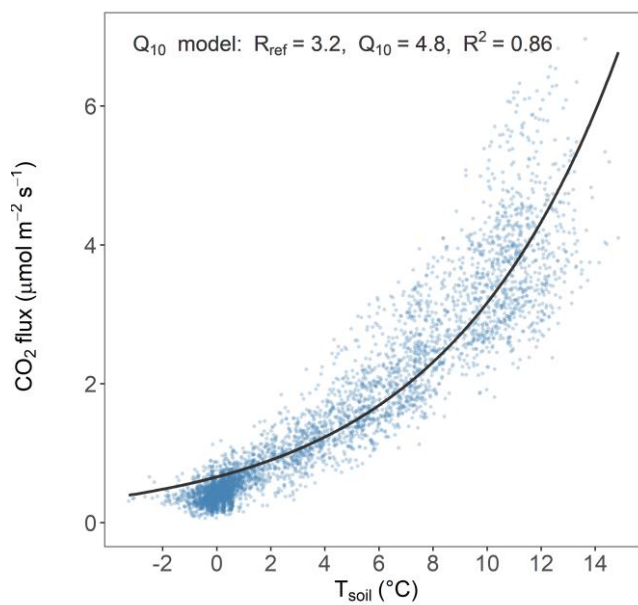
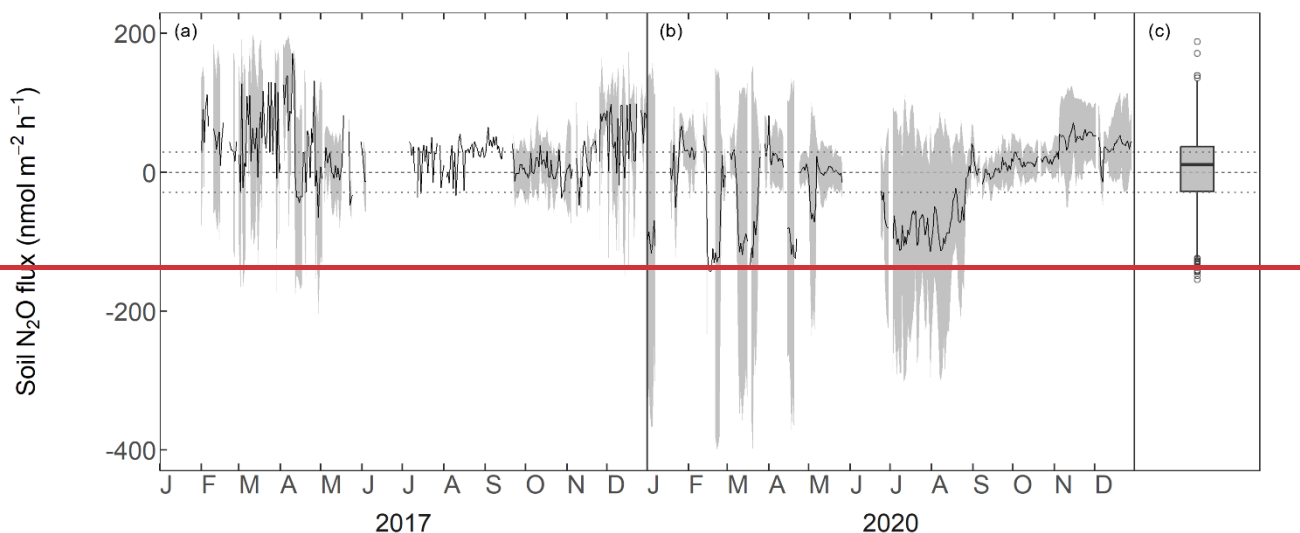


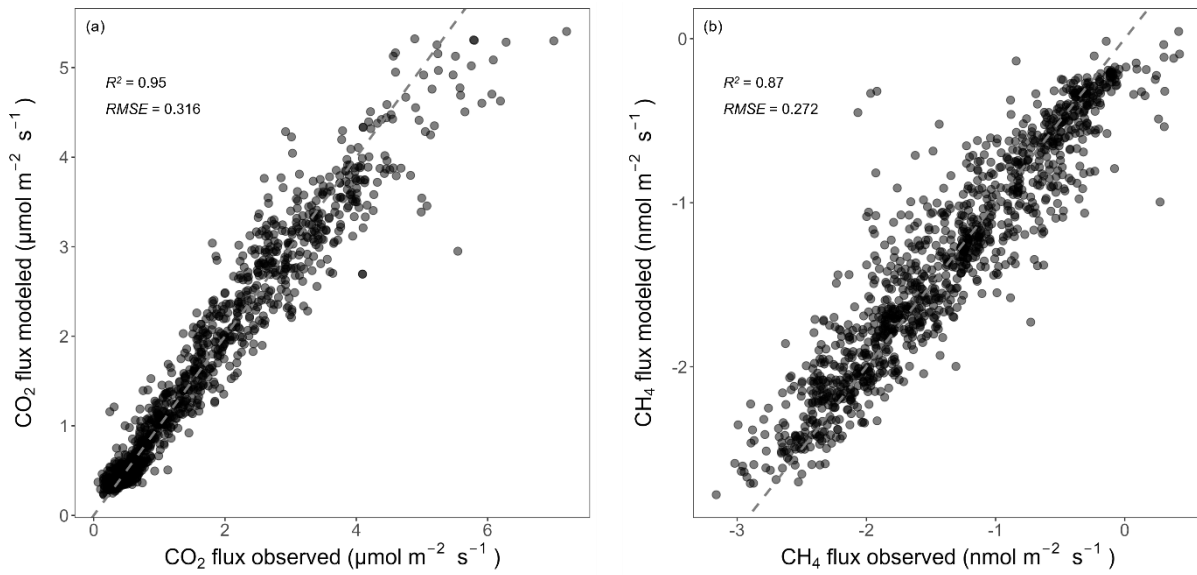
Fig. A.4: Q_{10} model showing the relationship of daily means of T_{soil} at 5 cm and forest-floor respiration of all chambers and years.



605 **Fig. A.1:** Forest floor N_2O fluxes ($\text{nmol m}^{-2} \text{h}^{-1}$) for the years 2017 (a) and 2020 (b). Black lines show means over four chambers, grey bands show standard deviations among four chambers. Boxplot showing distribution of means over four chambers (c). The dotted lines depict the minimum flux which could be detected by the Dual-Quantum-Cascade-Laser spectrometer.

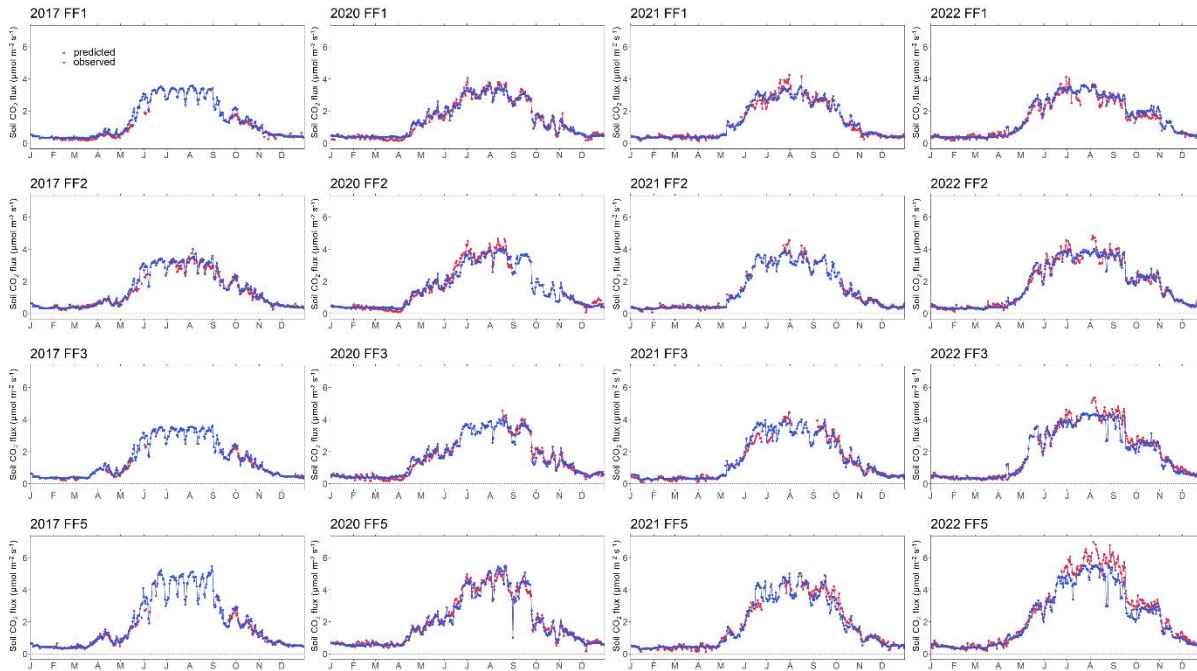
610 **Tab. A.31:** Details of random forest models used for driver analysis and gap-filling for different time periods (entire year, separately for seasons). Number of observations used to train the models (training set), the hyperparameters “mtry” and “ntree” as well as the R^2 values for observed vs. predicted test data are given. “mtry” specifies how many variables were randomly sampled as candidates at each split, “ntree” indicates the number of trees.

Gas	Time period	No. observations in training set	mtry	ntree	test R^2
CO_2	entire year	3111	10	2000	0.95
	spring	860	18	2000	0.94
	summer	623	14	2000	0.73
	autumn	836	14	2000	0.90
	winter	774	14	2000	0.63
CH_4	entire year	2799	14	2000	0.87
	spring	825	18	2000	0.80
	summer	520	18	2000	0.76
	autumn	772	10	2000	0.72
	winter	674	10	2000	0.73



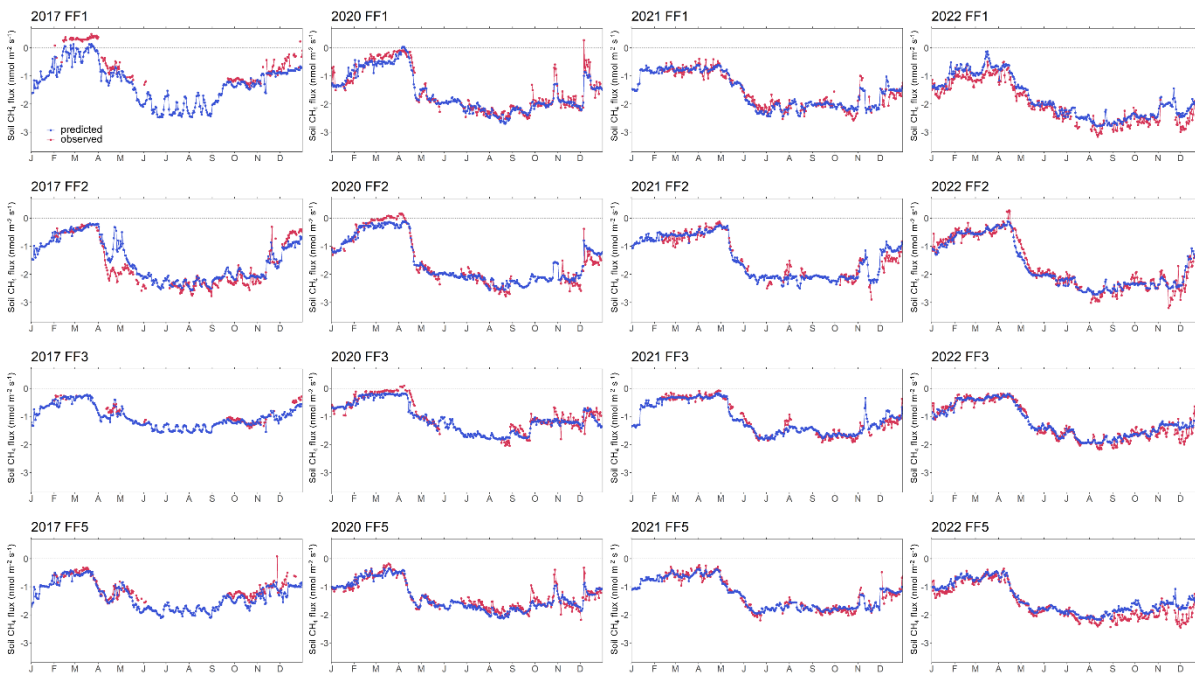
615

Fig. A.52: Relationships between observed and predicted **forest-floor** (a) **respiration** CO_2 and (b) CH_4 fluxes from the RF models used for gap filling (only showing test data). R^2 and RSME are given. Black dashed lines mark the 1:1 lines.



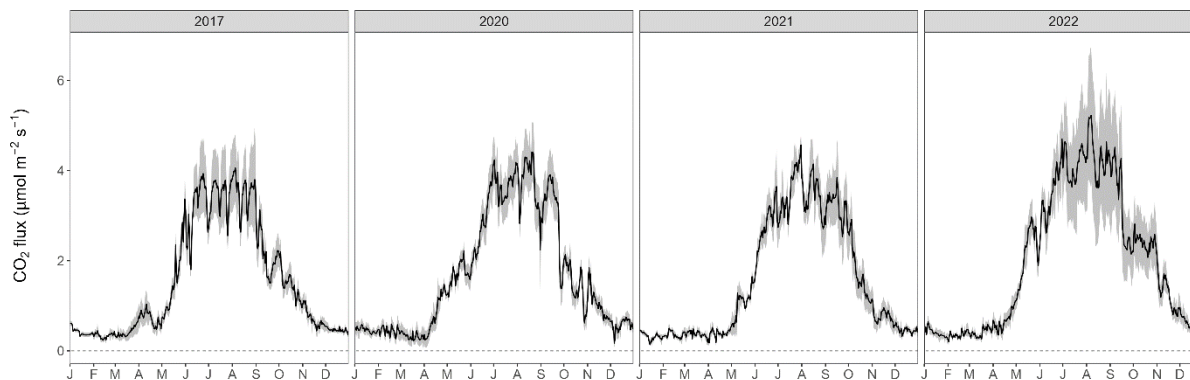
620

Fig. A.63: Time series of observed and predicted (using random forest model) forest-floor **CO_2 -respiration** fluxes for four years (2017, 2020–2022) and four chambers (FF1 to FF4).



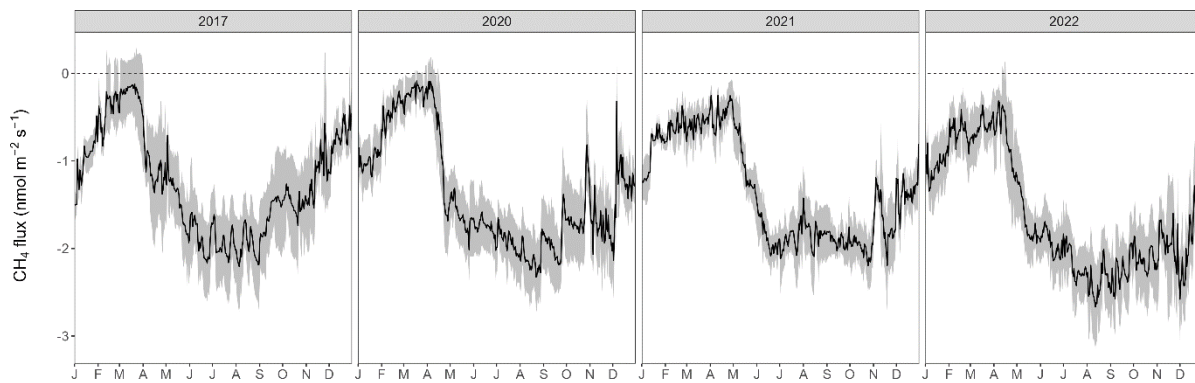
625

Fig. A.74: Time series of observed and predicted (using random forest model) forest-floor CH_4 fluxes for four years (2017, 2020–2022) and four chambers (FF1 to FF4).



630

Fig. A.85: Gap-filled CO_2 -forest-floor respiration fluxes over four years (grey area: min-max among four chambers).



635 Fig. A.96: Gap-filled **forest-floor** CH₄ fluxes over four years (grey area: min-max among four chambers).

References

- Amthor, J. S.: The McCree–de Wit–Penning de Vries–Thornley Respiration Paradigms: 30 Years Later, *Ann. Bot.*, 86, 1–20, <https://doi.org/10.1006/anbo.2000.1175>, 2000.
- 640 Anjileli, H., Huning, L. S., Moftakhari, Ashraf, S., Asanjan, A. A., Norouzi, H., and AghaKouchak, A.: Extreme heat events heighten soil respiration, *Sci. Rep.*, 11, 6632, <https://doi.org/10.1038/s41598-021-85764-8>
- Arrouays, D., Saby, N. P. A., Boukir, H., Jolivet, C., Ratié, C., Schrumpf, M., Merbold, L., Gielen, B., Gogo, S., Delpierre, N., Vincent, G., Klumpp, K., and Loustau, D.: Soil sampling and preparation for monitoring soil carbon, *Int. Agrophysics*, 32, 633–643, <https://doi.org/10.1515/intag-2017-0047>, 2018.
- 645 Barba, J., Cueva, A., Bahn, M., Barron-Gafford, G. A., Bond-Lamberty, B., Hanson, P. J., Jaimes, A., Kulmala, L., Pumpanen, J., Scott, R. L., Wohlfahrt, G., and Vargas, R.: Comparing ecosystem and soil respiration: Review and key challenges of tower-based and soil measurements, *Agric. For. Meteorol.*, 249, 434–443, <https://doi.org/10.1016/j.agrformet.2017.10.028>, 2018.
- Barba, J., Poyatos, R., and Vargas, R.: Automated measurements of greenhouse gases fluxes from tree stems and soils: magnitudes, patterns and drivers, *Sci. Rep.*, 9, 4005, <https://doi.org/10.1038/s41598-019-39663-8>, 2019.
- 650 Barrena, I., Menéndez, S., Duñabeitia, M., Merino, P., Florian Stange, C., Spott, O., González-Murua, C., and Estavillo, J. M.: Greenhouse gas fluxes (CO₂, N₂O and CH₄) from forest soils in the Basque Country: Comparison of different tree species and growth stages, *For. Ecol. Manag.*, 310, 600–611, <https://doi.org/10.1016/j.foreco.2013.08.065>, 2013.
- Barthel, M., Bauters, M., Baumgartner, S., Drake, T. W., Bey, N. M., Bush, G., Boeckx, P., Botefa, C. I., Dériaz, N., Ekamba, G. L., Gallarotti, N., Mbayu, F. M., Mugula, J. K., Makelele, I. A., Mbongo, C. E., Mohn, J., Manda, J. Z., Mpambi, D. M., Ntaboba, L. C., Rukeza, M. B., Spencer, R. G. M., Summerauer, L., Vanlauwe, B., Van Oost, K., Wolf, B., and Six, J.: Low N₂O and variable CH₄ fluxes from tropical forest soils of the Congo Basin, *Nat. Commun.*, 13, 330, <https://doi.org/10.1038/s41467-022-27978-6>, 2022.
- Basiliko, N., Knowles, R., and Moore, T. R.: Roles of moss species and habitat in methane consumption potential in a northern peatland, *Wetlands*, 24, 178–185, [https://doi.org/10.1672/0277-5212\(2004\)024\[0178:ROMSAH\]2.0.CO;2](https://doi.org/10.1672/0277-5212(2004)024[0178:ROMSAH]2.0.CO;2), 2004.

- 660 Blankinship, J. C., McCorkle, E. P., Meadows, M. W., and Hart, S. C.: Quantifying the legacy of snowmelt timing on soil greenhouse gas emissions in a seasonally dry montane forest, *Glob. Change Biol.*, 24, 5933–5947, <https://doi.org/10.1111/gcb.14471>, 2018.
- Bond-Lamberty, B., Bailey, V. L., Chen, M., Gough, C. M., and Vargas, R.: Globally rising soil heterotrophic respiration over recent decades, *Nature*, 560, 80–83, <https://doi.org/10.1038/s41586-018-0358-x>, 2018.
- 665 Borken, W., Davidson, E. A., Savage, K., Sundquist, E. T., and Steudler, P.: Effect of summer throughfall exclusion, summer drought, and winter snow cover on methane fluxes in a temperate forest soil, *Soil Biol. Biochem.*, 38, 1388–1395, <https://doi.org/10.1016/j.soilbio.2005.10.011>, 2006.
- Brümmer, C., Lyshede, B., Lempio, D., Delorme, J.-P., Rüffer, J. J., Fuß, R., Moffat, A. M., Hurkuck, M., Ibrom, A., Ambus, P., Flessa, H., and Kutsch, W. L.: Gas chromatography vs. quantum cascade laser-based N₂O flux measurements using a novel chamber design, *Biogeosciences*, 14, 1365–1381, <https://doi.org/10.5194/bg-14-1365-2017>, 2017.
- 670 Butterbach-Bahl, K., Baggs, E. M., Dannenmann, M., Kiese, R., and Zechmeister-Boltenstern, S.: Nitrous oxide emissions from soils: how well do we understand the processes and their controls?, *Philos. Trans. R. Soc. B Biol. Sci.*, 368, 20130122, <https://doi.org/10.1098/rstb.2013.0122>, 2013.
- CH2018: CH2018 – Climate Scenarios for Switzerland, Technical Report, National Centre for Climate Services, Zurich, 2018.
- 675 Chapuis-Lardy, L., Wrage, N., Metay, A., Chotte, J.-L., and Bernoux, M.: Soils, a sink for N₂O? A review, *Glob. Change Biol.*, 13, 1–17, <https://doi.org/10.1111/j.1365-2486.2006.01280.x>, 2007.
- Chen, W., Wang, S., Wang, J., Xia, J., Luo, Y., Yu, G., and Niu, S.: Evidence for widespread thermal optimality of ecosystem respiration, *Nat. Ecol. Evol.*, 7, 1379–1387, <https://doi.org/10.1038/s41559-023-02121-w>, 2023.
- Danielson, R. E. and Sutherland, P. L.: Porosity, in: *SSSA Book Series*, edited by: Klute, A., Soil Science Society of America, American Society of Agronomy, Madison, WI, USA, 443–461, <https://doi.org/10.2136/sssabookser5.1.2ed.c18>, 2018.
- Davidson, E. A., Janssens, I. A., and Luo, Y.: On the variability of respiration in terrestrial ecosystems: moving beyond Q_{10} : On the variability of respiration in terrestrial ecosystems, *Glob. Change Biol.*, 12, 154–164, <https://doi.org/10.1111/j.1365-2486.2005.01065.x>, 2006.
- 685 Debeer, D. and Strobl, C.: Conditional permutation importance revisited, *BMC Bioinformatics*, 21, 307, <https://doi.org/10.1186/s12859-020-03622-2>, 2020.
- Debeer, D., Hothorn, T., and Strobl, C.: permimp: Conditional Permutation Importance, 2021.
- Dutaur, L. and Verchot, L. V.: A global inventory of the soil CH₄ sink, *Glob. Biogeochem. Cycles*, 21, GB4013, <https://doi.org/10.1029/2006GB002734>, 2007.
- 690 Fest, B. J., Livesley, S. J., Drösler, M., van Gorsel, E., and Arndt, S. K.: Soil–atmosphere greenhouse gas exchange in a cool, temperate Eucalyptus delegatensis forest in south-eastern Australia, *Agric. For. Meteorol.*, 149, 393–406, <https://doi.org/10.1016/j.agrformet.2008.09.007>, 2009.
- 695 Friedlingstein, P., O’Sullivan, M., Jones, M. W., Andrew, R. M., Bakker, D. C. E., Hauck, J., Landschützer, P., Le Quééré, C., Luijkx, I. T., Peters, G. P., Peters, W., Pongratz, J., Schwingshackl, C., Sitch, S., Canadell, J. G., Ciais, P., Jackson, R. B., Alin, S. R., Anthoni, P., Barbero, L., Bates, N. R., Becker, M., Bellouin, N., Decharme, B., Bopp, L., Brasika, I. B. M., Cadule, P., Chamberlain, M. A., Chandra, N., Chau, T.-T.-T., Chevallier, F., Chini, L. P., Cronin, M., Dou, X., Enyo, K., Evans, W.,

- Falk, S., Feely, R. A., Feng, L., Ford, D. J., Gasser, T., Ghattas, J., Gkritzalis, T., Grassi, G., Gregor, L., Gruber, N., Gürses, Ö., Harris, I., Hefner, M., Heinke, J., Houghton, R. A., Hurtt, G. C., Iida, Y., Ilyina, T., Jacobson, A. R., Jain, A., Jarníková, T., Jersild, A., Jiang, F., Jin, Z., Joos, F., Kato, E., Keeling, R. F., Kennedy, D., Klein Goldewijk, K., Knauer, J., Korsbakken, J. I., Körtzinger, A., Lan, X., Lefèvre, N., Li, H., Liu, J., Liu, Z., Ma, L., Marland, G., Mayot, N., McGuire, P. C., McKinley, G. A., Meyer, G., Morgan, E. J., Munro, D. R., Nakaoka, S.-I., Niwa, Y., O'Brien, K. M., Olsen, A., Omar, A. M., Ono, T., Paulsen, M., Pierrot, D., Pockock, K., Poulter, B., Powis, C. M., Rehder, G., Resplandy, L., Robertson, E., Rödenbeck, C., Rosan, T. M., Schwinger, J., Séférian, R., et al.: Global Carbon Budget 2023, *Earth Syst. Sci. Data*, 15, 5301–5369, <https://doi.org/10.5194/essd-15-5301-2023>, 2023.
- 705 Fuentes, S., Palmer, A. R., Taylor, D., Zeppel, M., Whitley, R., and Eamus, D.: An automated procedure for estimating the leaf area index (LAI) of woodland ecosystems using digital imagery, MATLAB programming and its application to an examination of the relationship between remotely sensed and field measurements of LAI, *Funct. Plant Biol.*, 35, 1070, <https://doi.org/10.1071/FP08045>, 2008.
- 710 Gao, D., Hagedorn, F., Zhang, L., Liu, J., Qu, G., Sun, J., Peng, B., Fan, Z., Zheng, J., Jiang, P., and Bai, E.: Small and transient response of winter soil respiration and microbial communities to altered snow depth in a mid-temperate forest, *Appl. Soil Ecol.*, 130, 40–49, <https://doi.org/10.1016/j.apsoil.2018.05.010>, 2018.
- Gaumont-Guay, D., Black, T. A., Barr, A. G., Griffis, T. J., Jassal, R. S., Krishnan, P., Grant, N., and Nesic, Z.: Eight years of forest-floor CO₂ exchange in a boreal black spruce forest: Spatial integration and long-term temporal trends, *Agric. For. Meteorol.*, 184, 25–35, <https://doi.org/10.1016/j.agrformet.2013.08.010>, 2014.
- 715 Gharun, M., Klesse, S., Tomlinson, G., Waldner, P., Stocker, B., Rihm, B., Siegwolf, R., and Buchmann, N.: Effect of nitrogen deposition on centennial forest water-use efficiency, *Environ. Res. Lett.*, 16, 114036, <https://doi.org/10.1088/1748-9326/ac30f9>, 2021.
- Goldberg, S. D. and Gebauer, G.: N₂O and NO fluxes between a Norway spruce forest soil and atmosphere as affected by prolonged summer drought, *Soil Biol.*, 41, 1986–1995, <https://doi.org/10.1016/j.soilbio.2009.07.001>, 2009.
- 720 Goldberg, S. D., Borken, W., and Gebauer, G.: N₂O emission in a Norway spruce forest due to soil frost: concentration and isotope profiles shed a new light on an old story, *Biogeochemistry*, 97, 21–30, <https://doi.org/10.1007/s10533-009-9294-z>, 2010.
- Goldman, M. B., Groffman, P. M., Pouyat, R. V., McDonnell, M. J., and Pickett, S. T. A.: CH₄ uptake and N availability in forest soils along an urban to rural gradient, *Soil Biol. Biochem.*, 27, 281–286, [https://doi.org/10.1016/0038-0717\(94\)00185-4](https://doi.org/10.1016/0038-0717(94)00185-4), 1995.
- 725 Goldstein, A., Kapelner, A., Bleich, J., and Pitkin, E.: Peeking inside the black box: Visualizing statistical learning with plots of individual conditional expectation, *J. Comput. Graph. Stat.*, 24, 44–65, <https://doi.org/10.1080/10618600.2014.907095>, 2015.
- Greenwell, B., M.: pdp: An R package for constructing partial dependence plots, *R J.*, 9, 421, <https://doi.org/10.32614/RJ-2017-016>, 2017.
- 730 Groffman, P. M., Hardy, J. P., Driscoll, C. T., and Fahey, T. J.: Snow depth, soil freezing, and fluxes of carbon dioxide, nitrous oxide and methane in a northern hardwood forest, *Glob. Change Biol.*, 12, 1748–1760, <https://doi.org/10.1111/j.1365-2486.2006.01194.x>, 2006.

- 735 Guo, C., Zhang, L., Li, S., Li, Q., and Dai, G.: Comparison of Soil Greenhouse Gas Fluxes during the Spring Freeze–Thaw Period and the Growing Season in a Temperate Broadleaved Korean Pine Forest, Changbai Mountains, China, *Forests*, 11, 1135, 2020.
- Hahn, M., Gartner, K., and Zechmeister-Boltenstern, S.: Greenhouse gas emissions (N₂O, CO₂ and CH₄) from three forest soils near Vienna (Austria) with different water and nitrogen regimes, *Bodenkultur*, 51, 115–125, 2000.
- 740 Hanson, P. J., Edwards, N. T., Garten, C. T., and Andrews, J. A.: Separating root and soil microbial contributions to soil respiration: A review of methods and observations, *Biogeochemistry*, 48, 115–146, <https://doi.org/10.1023/A:1006244819642>, 2000.
- Högberg, P., Nordgren, A., Buchmann, N., Taylor, A. F. S., Ekblad, A., Högberg, M. N., Nyberg, G., Ottosson-Löfvenius, M., and Read, D. J.: Large-scale forest girdling shows that current photosynthesis drives soil respiration, *Nature*, 411, 789–792, <https://doi.org/10.1038/35081058>, 2001.
- 745 Hopfensperger, K. N., Gault, C. M., and Groffman, P. M.: Influence of plant communities and soil properties on trace gas fluxes in riparian northern hardwood forests, *For. Ecol. Manag.*, 258, 2076–2082, <https://doi.org/10.1016/j.foreco.2009.08.004>, 2009.
- Hutchinson, G. L. and Mosier, A. R.: Improved Soil Cover Method for Field Measurement of Nitrous Oxide Fluxes, *Soil Sci. Soc. Am. J.*, 45, 311–316, <https://doi.org/10.2136/sssaj1981.03615995004500020017x>, 1981.
- Ingestad, T.: Studies on the Nutrition of Forest Tree Seedlings. II Mineral Nutrition of Spruce, *Physiol. Plant.*, 568–593, 1959.
- 750 IPCC: Climate Change 2021: The Physical Science Basis. Contribution of Working Group I to the Sixth Assessment Report of the Intergovernmental Panel on Climate Change, Cambridge University Press, Cambridge, United Kingdom and New York, NY, USA, 2021.
- 755 Janssens, I. A., Lankreijer, H., Matteucci, G., Kowalski, A. S., Buchmann, N., Epron, D., Pilegaard, K., Kutsch, W., Longdoz, B., Grünwald, T., Montagnani, L., Dore, S., Rebmann, C., Moors, E. J., Grelle, A., Rannik, Ü., Morgenstern, K., Oltchev, S., Clement, R., Guðmundsson, J., Minerbi, S., Berbigier, P., Ibrom, A., Moncrieff, J., Aubinet, M., Bernhofer, C., Jensen, N. O., Vesala, T., Granier, A., Schulze, E.-D., Lindroth, A., Dolman, A. J., Jarvis, P. G., Ceulemans, R., and Valentini, R.: Productivity overshadows temperature in determining soil and ecosystem respiration across European forests, *Glob. Change Biol.*, 7, 269–278, <https://doi.org/10.1046/j.1365-2486.2001.00412.x>, 2001.
- 760 Jörg, S.: Böden im Seehornwald bei Davos und deren Vorrat an Kohlenstoff und Stickstoff. Diplomarbeit, Zürcher Hochschule für Angewandte Wissenschaften, Zürcher Hochschule für Angewandte Wissenschaften, Zurich, 79 pp., 2008.
- Kim, Y., Kodama, Y., and Fochesatto, G. J.: Environmental factors regulating winter CO₂ flux in snow-covered black forest soil of Interior Alaska, *Geochem. J.*, 51, 359–371, <https://doi.org/10.2343/geochemj.2.0475>, 2017.
- 765 Klein, G., Vitasse, Y., Rixen, C., Marty, C., and Rebetez, M.: Shorter snow cover duration since 1970 in the Swiss Alps due to earlier snowmelt more than to later snow onset, *Clim. Change*, 139, 637–649, <https://doi.org/10.1007/s10584-016-1806-y>, 2016.
- Krause, K., Niklaus, P. A., and Schleppei, P.: Soil-atmosphere fluxes of the greenhouse gases CO₂, CH₄ and N₂O in a mountain spruce forest subjected to long-term N addition and to tree girdling, *Agric. For. Meteorol.*, 181, 61–68, <https://doi.org/10.1016/j.agrformet.2013.07.007>, 2013.

- 770 Kuhn, M.: Building Predictive Models in R Using the caret Package, *J. Stat. Softw.*, 28, 1–26, <https://doi.org/10.18637/jss.v028.i05>, 2008.
- 775 Lembrechts, J. J., van den Hoogen, J., Aalto, J., Ashcroft, M. B., De Frenne, P., Kemppinen, J., Kopecký, M., Luoto, M., Maclean, I. M. D., Crowther, T. W., Bailey, J. J., Haesen, S., Klinges, D. H., Niittynen, P., Scheffers, B. R., Van Meerbeek, K., Aartsma, P., Abdalaze, O., Abedi, M., Aerts, R., Ahmadian, N., Ahrends, A., Alatalo, J. M., Alexander, J. M., Allonsius, C. N., Altman, J., Ammann, C., Andres, C., Andrews, C., Ardö, J., Arriga, N., Arzac, A., Aschero, V., Assis, R. L., Assmann, J. J., Bader, M. Y., Bahalkeh, K., Barančok, P., Barrio, I. C., Barros, A., Barthel, M., Basham, E. W., Bauters, M., Bazzichetto, M., Marchesini, L. B., Bell, M. C., Benavides, J. C., Benito Alonso, J. L., Berauer, B. J., Bjerke, J. W., Björk, R. G., Björkman, M. P., Björnsdóttir, K., Blonder, B., Boeckx, P., Boike, J., Bokhorst, S., Brum, B. N. S., Brúna, J., Buchmann, N., Buysse, P., Camargo, J. L., Campoe, O. C., Candan, O., Canessa, R., Cannone, N., Carbognani, M., Carnicer, J., Casanova-Katny, A., Cesarz, S., Chojnicki, B., Choler, P., Chown, S. L., Cifuentes, E. F., Čiliak, M., Contador, T., Convey, P., Cooper, E. J., 780 Cremonese, E., Curasi, S. R., Curtis, R., Cutini, M., Dahlberg, C. J., Daskalova, G. N., de Pablo, M. A., Della Chiesa, S., Dengler, J., Deronde, B., Descombes, P., Di Cecco, V., Di Musciano, M., Dick, J., Dimarco, R. D., Dolezal, J., Dorrepaal, E., Dušek, J., Eisenhauer, N., Eklundh, L., Erickson, T. E., et al.: Global maps of soil temperature, *Glob. Change Biol.*, 28, 3110–3144, <https://doi.org/10.1111/gcb.16060>, 2022.
- 785 Liu, S., Schlöter, M., and Brüggemann, N.: Accumulation of NO₂⁻ during periods of drying stimulates soil N₂O emissions during subsequent rewetting: Nitrite stimulates N₂O emissions during rewetting, *Eur. J. Soil Sci.*, 69, 936–946, <https://doi.org/10.1111/ejss.12683>, 2018.
- Luedeling, E. and Fernandez, E.: chillR: Statistical methods for phenology analysis in temperate fruit, 2022.
- 790 Luo, G. J., Brüggemann, N., Wolf, B., Gasche, R., Grote, R., and Butterbach-Bahl, K.: Decadal variability of soil CO₂, NO, N₂O, and CH₄ fluxes at the Höglwald Forest, Germany, *Biogeosciences*, 9, 1741–1763, <https://doi.org/10.5194/BG-9-1741-2012>, 2011.
- Luo, G. J., Kiese, R., Wolf, B., and Butterbach-Bahl, K.: Effects of soil temperature and moisture on methane uptake and nitrous oxide emissions across three different ecosystem types, *Biogeosciences*, 10, 3205–3219, <https://doi.org/10.5194/bg-10-3205-2013>, 2013.
- 795 Martins, C. S. C., Nazaries, L., Delgado-Baquerizo, M., Macdonald, C. A., Anderson, I. C., Hobbie, S. E., Venterea, R. T., Reich, P. B., and Singh, B. K.: Identifying environmental drivers of greenhouse gas emissions under warming and reduced rainfall in boreal–temperate forests, *Funct. Ecol.*, 31, 2356–2368, <https://doi.org/10.1111/1365-2435.12928>, 2017.
- Martinson, G. O., Müller, A. K., Matson, A. L., Corre, M. D., and Veldkamp, E.: Nitrogen and Phosphorus Control Soil Methane Uptake in Tropical Montane Forests, *J. Geophys. Res. Biogeosciences*, 126(8), e2020JG005970, <https://doi.org/10.1029/2020JG005970>, 2021.
- 800 McManus, J. B., Nelson, D. D., Herndon, S. C., Shorter, J. H., Zahniser, M. S., Blaser, S., Hvozďara, L., Muller, A., Giovannini, M., and Faist, J.: Comparison of cw and pulsed operation with a TE-cooled quantum cascade infrared laser for detection of nitric oxide at 1900 cm⁻¹, *Appl. Phys. B*, 85, 235–241, <https://doi.org/10.1007/s00340-006-2407-7>, 2006.
- 805 Mitra, B., Miao, G., Minick, K., McNulty, S. G., Sun, G., Gavazzi, M., King, J. S., and Noormets, A.: Disentangling the Effects of Temperature, Moisture, and Substrate Availability on Soil CO₂ Efflux, *J. Geophys. Res. Biogeosciences*, 124, 2060–2075, <https://doi.org/10.1029/2019JG005148>, 2019.
- Ni, X. and Groffman, P. M.: Declines in methane uptake in forest soils, *Proc. Natl. Acad. Sci.*, 115, 8587–8590, <https://doi.org/10.1073/pnas.1807377115>, 2018.

- Nissan, A., Alcolombri, U., Peleg, N., Galili, N., Jimenez-Martinez, J., Molnar, P., and Holzner, M.: Global warming accelerates soil heterotrophic respiration, *Nat. Commun.*, 14, 3452, <https://doi.org/10.1038/s41467-023-38981-w>, 2023.
- 810 Pang, J., Peng, C., Wang, X., Zhang, H., and Zhang, S.: Soil-atmosphere exchange of carbon dioxide, methane and nitrous oxide in temperate forests along an elevation gradient in the Qinling Mountains, China, *Plant Soil*, 488, 325–342, <https://doi.org/10.1007/s11104-023-05967-y>, 2023.
- Papen, H. and Butterbach-Bahl, K.: A 3-year continuous record of nitrogen trace gas fluxes from untreated and limed soil of a N-saturated spruce and beech forest ecosystem in Germany: 1. N₂O emissions, *J. Geophys. Res. Atmospheres*, 104, 18487–18503, <https://doi.org/10.1029/1999JD900293>, 1999.
- 815 Pavelka, M., Acosta, M., Kiese, R., Altimir, N., Brümmer, C., Crill, P., Darenova, E., Fuß, R., Gielen, B., Graf, A., Klemedtsson, L., Lohila, A., Longdoz, B., Lindroth, A., Nilsson, M., Jiménez, S. M., Merbold, L., Montagnani, L., Peichl, M., Pihlatie, M., Pumpanen, J., Ortiz, P. S., Silvennoinen, H., Skiba, U., Vestin, P., Weslien, P., Janous, D., and Kutsch, W.: Standardisation of chamber technique for CO₂, N₂O and CH₄ fluxes measurements from terrestrial ecosystems, *Int. Agrophysics*, 32, 569–587, <https://doi.org/10.1515/intag-2017-0045>, 2018.
- 820 Pilegaard, K., Mikkelsen, T. N., Beier, C., Jensen, N., Ambus, P., and Ro-Poulsen, H.: Field measurements of atmosphere–biosphere interactions in a Danish beech forest, *Boreal Environ. Res.*, 8, 315–333, 2003.
- R Core Team: R: A language and environment for statistical computing, R Foundation for Statistical Computing, Vienna, Austria, 2022.
- 825 Reichstein, M., Bahn, M., Ciais, P., Frank, D., Mahecha, M. D., Seneviratne, S. I., Zscheischler, J., Beer, C., Buchmann, N., Frank, D. C., Papale, D., Rammig, A., Smith, P., Thonicke, K., van der Velde, M., Vicca, S., Walz, A., and Wattenbach, M.: Climate extremes and the carbon cycle, *Nature*, 500, 287–295, <https://doi.org/10.1038/nature12350>, 2013.
- Reinmann, A. B. and Templer, P. H.: Increased soil respiration in response to experimentally reduced snow cover and increased soil freezing in a temperate deciduous forest, *Biogeochemistry*, 140, 359–371, <https://doi.org/10.1007/s10533-018-0497-z>, 2018.
- 830 Richardson, A. D., Hollinger, D. Y., Shoemaker, J. K., Hughes, H., Savage, K., and Davidson, E. A.: Six years of ecosystem-atmosphere greenhouse gas fluxes measured in a sub-boreal forest, *Sci. Data*, 6, 117, <https://doi.org/10.1038/s41597-019-0119-1>, 2019.
- Robette, N.: moreparty: A toolbox for conditional inference trees and random forests, 2023.
- 835 Ruehr, N. K., Knohl, A., and Buchmann, N.: Environmental variables controlling soil respiration on diurnal, seasonal and annual time-scales in a mixed mountain forest in Switzerland, *Biogeochemistry*, 98, 153–170, <https://doi.org/10.1007/s10533-009-9383-z>, 2010.
- Rütting, T., Björnsne, A.-K., Weslien, P., Kasimir, Å., and Klemedtsson, L.: Low Nitrous Oxide Emissions in a Boreal Spruce Forest Soil, Despite Long-Term Fertilization, *Front. For. Glob. Change*, 4, <https://doi.org/10.3389/ffgc.2021.710574>, 2021.
- 840 Saby, N., Loubet, B., Goydarag, M. G., Papale, D., Arrouays, D., and Lafont, S.: Computing C Stock for one ICOS Site, ICOS Ecosystem Thematic Centre, 2023.
- Saunois, M., Stavert, A. R., Poulter, B., Bousquet, P., Canadell, J. G., Jackson, R. B., Raymond, P. A., Dlugokencky, E. J., Houweling, S., Patra, P. K., Ciais, P., Arora, V. K., Bastviken, D., Bergamaschi, P., Blake, D. R., Brailsford, G., Bruhwiler, L., Carlson, K. M., Carrol, M., Castaldi, S., Chandra, N., Crevoisier, C., Crill, P. M., Covey, K., Curry, C. L., Etiope, G.,

- 845 Frankenberg, C., Gedney, N., Hegglin, M. I., Höglund-Isaksson, L., Hugelius, G., Ishizawa, M., Ito, A., Janssens-Maenhout, G., Jensen, K. M., Joos, F., Kleinen, T., Krummel, P. B., Langenfelds, R. L., Laruelle, G. G., Liu, L., Machida, T., Maksyutov, S., McDonald, K. C., McNorton, J., Miller, P. A., Melton, J. R., Morino, I., Müller, J., Murguía-Flores, F., Naik, V., Niwa, Y., Noce, S., O'Doherty, S., Parker, R. J., Peng, C., Peng, S., Peters, G. P., Prigent, C., Prinn, R., Ramonet, M., Regnier, P., Riley, W. J., Rosentretter, J. A., Segers, A., Simpson, I. J., Shi, H., Smith, S. J., Steele, L. P., Thornton, B. F., Tian, H., Tohjima, Y.,
- 850 Tubiello, F. N., Tsuruta, A., Viovy, N., Voulgarakis, A., Weber, T. S., van Weele, M., van der Werf, G. R., Weiss, R. F., Worthy, D., Wunch, D., Yin, Y., Yoshida, Y., Zhang, W., Zhang, Z., Zhao, Y., Zheng, B., Zhu, Q., Zhu, Q., and Zhuang, Q.: The Global Methane Budget 2000–2017, *Earth Syst. Sci. Data*, 12, 1561–1623, <https://doi.org/10.5194/essd-12-1561-2020>, 2020.
- Schaufler, G., Kitzler, B., Schindlbacher, A., Skiba, U., Sutton, M., and Zechmeister-Boltenstern, S.: Greenhouse gas emissions from European soils under different land use: effects of soil moisture and temperature, *Eur. J. Soil Sci.*, 61, 683–696, <https://doi.org/10.1111/j.1365-2389.2010.01277.x>, 2010.
- Schindlbacher, A., Zechmeister-Boltenstern, S., Glatzel, G., and Jandl, R.: Winter soil respiration from an Austrian mountain forest, *Agric. For. Meteorol.*, 146, 205–215, <https://doi.org/10.1016/j.agrformet.2007.06.001>, 2007.
- Schindlbacher, A., Jandl, R., and Schindlbacher, S.: Natural variations in snow cover do not affect the annual soil CO₂ from a mid-elevation temperate forest, *Glob. Change Biol.*, 20, 622–632, <https://doi.org/10.1111/gcb.12367>, 2014.
- Schulze, E.-D. (Ed.) Caldwell, M. M., Heldmaier, G., Lange, O. L., Mooney, H. A., Schulze, E.-D., and Sommer, U.: Carbon and Nitrogen Cycling in European Forest Ecosystems, Springer Berlin Heidelberg, Berlin, Heidelberg, <https://doi.org/10.1007/978-3-642-57219-7>, 2000.
- 865 Scott-Denton, L. E., Rosenstiel, T. N., and Monson, R. K.: Differential controls by climate and substrate over the heterotrophic and rhizospheric components of soil respiration: Controls over soil respiration, *Glob. Change Biol.*, 12, 205–216, <https://doi.org/10.1111/j.1365-2486.2005.01064.x>, 2006.
- Sommerfeld, R. A., Mosier, A. R., and Musselman, R. C.: CO₂, CH₄ and N₂O flux through a Wyoming snowpack and implications for global budgets, *Nature*, 361, 140–142, <https://doi.org/10.1038/361140a0>, 1993.
- Song, Y., Zou, Y., Wang, G., and Yu, X.: Altered soil carbon and nitrogen cycles due to the freeze-thaw effect: A meta-analysis, *Soil Biol. Biochem.*, 109, 35–49, <https://doi.org/10.1016/j.soilbio.2017.01.020>, 2017.
- 870 Strobl, C., Boulesteix, A.-L., Zeileis, A., and Hothorn, T.: Bias in random forest variable importance measures: Illustrations, sources and a solution, *BMC Bioinformatics*, 8, 25, <https://doi.org/10.1186/1471-2105-8-25>, 2007.
- Strobl, C., Boulesteix, A.-L., Kneib, T., Augustin, T., and Zeileis, A.: Conditional variable importance for random forests, *BMC Bioinformatics*, 9, 307, <https://doi.org/10.1186/1471-2105-9-307>, 2008.
- 875 Thimonier, A., Graf Pannatier, E., Schmitt, M., Waldner, P., Walthert, L., Schleppei, P., Dobbertin, M., and Kräuchi, N.: Does exceeding the critical loads for nitrogen alter nitrate leaching, the nutrient status of trees and their crown condition at Swiss Long-term Forest Ecosystem Research (LWF) sites?, *Eur. J. For. Res.*, 443–461, <https://doi.org/10.1007/s10342-009-0328-9>, 2010.
- Thimonier, A., Kosonen, Z., Braun, S., Rihm, B., Schleppei, P., Schmitt, M., Seitler, E., Waldner, P., and Thöni, L.: Total deposition of nitrogen in Swiss forests: comparison of assessment methods and evaluation of changes over two decades, *Atmos. Environ.*, 335–350, <https://doi.org/10.1016/j.atmosenv.2018.10.051>, 2019.
- 880 Tschopp, T.: Zur Geschichte des Seehornwaldes in Davos. Praktikumsarbeit, WSL, Birmensdorf, 2012.

- Ueyama, M., Takeuchi, R., Takahashi, Y., Ide, R., Ataka, M., Kosugi, Y., Takahashi, K., and Saigusa, N.: Methane uptake in a temperate forest soil using continuous closed-chamber measurements, *Agric. For. Meteorol.*, 213, 1–9, 885 <https://doi.org/10.1016/j.agrformet.2015.05.004>, 2015.
- Ullah, S., Frasier, R., Pelletier, L., and Moore, T. R.: Greenhouse gas fluxes from boreal forest soils during the snow-free period in Quebec, Canada, *Can. J. For. Res.*, 39, 666–680, <https://doi.org/10.1139/X08-209>, 2009.
- Von Arnold, K., Weslien, P., Nilsson, M., Svensson, B. H., and Klemmedtsson, L.: Fluxes of CO₂, CH₄ and N₂O from drained coniferous forests on organic soils, *For. Ecol. Manag.*, 210, 239–254, <https://doi.org/10.1016/j.foreco.2005.02.031>, 2005.
- 890 Wang, C., Han, Y., Chen, J., Wang, X., Zhang, Q., and Bond-Lamberty, B.: Seasonality of soil CO₂ efflux in a temperate forest: Biophysical effects of snowpack and spring freeze–thaw cycles, *Agric. For. Meteorol.*, 177, 83–92, <https://doi.org/10.1016/j.agrformet.2013.04.008>, 2013.
- Wen, Y., Corre, M. D., Schrell, W., and Veldkamp, E.: Gross N₂O emission and gross N₂O uptake in soils under temperate spruce and beech forests, *Soil Biol. Biochem.*, 112, 228–236, <https://doi.org/10.1016/j.soilbio.2017.05.011>, 2017.
- 895 Wu, X., Zang, S., Ma, D., Ren, J., Chen, Q., and Dong, X.: Emissions of CO₂, CH₄, and N₂O Fluxes from Forest Soil in Permafrost Region of Daxing’an Mountains, Northeast China, *Int. J. Environ. Res. Public Health*, 16, 2999, <https://doi.org/10.3390/ijerph16162999>, 2019.
- Xie, J., Kneubühler, M., Garonna, I., Notarnicola, C., De Gregorio, L., De Jong, R., Chimani, B., and Schaepman, M. E.: Altitude-dependent influence of snow cover on alpine land surface phenology: Snow cover and Alpine phenology, *J. Geophys. Res. Biogeosciences*, 122, 1107–1122, <https://doi.org/10.1002/2016JG003728>, 2017.
- 900 Xu, Z., Zhou, F., Yin, H., and Liu, Q.: Winter soil CO₂ efflux in two contrasting forest ecosystems on the eastern Tibetan Plateau, China, *J. For. Res.*, 26, 679–686, <https://doi.org/10.1007/s11676-015-0120-2>, 2015.
- Yu, L., Huang, Y., Zhang, W., Li, T., and Sun, W.: Methane uptake in global forest and grassland soils from 1981 to 2010, *Sci. Total Environ.*, 607–608, 1163–1172, <https://doi.org/10.1016/j.scitotenv.2017.07.082>, 2017.
- 905 Yuste, J. C., Nagy, M., Janssens, I. A., Carrara, A., and Ceulemans, R.: Soil respiration in a mixed temperate forest and its contribution to total ecosystem respiration, *Tree Physiol.*, 25, 609–619, <https://doi.org/10.1093/treephys/25.5.609>, 2005.
- Zielis, S., Etzold, S., Zweifel, R., Eugster, W., Haeni, M., and Buchmann, N.: NEP of a Swiss subalpine forest is significantly driven not only by current but also by previous year’s weather, *Biogeosciences*, 11, 1627–1635, <https://doi.org/10.5194/bg-11-1627-2014>, 2014.